Supplementary Materials

Table of contents

No.	Legend	Page
Figure S1.	^{1}H NMR spectrum of solidagoic acid J (**1**) ($CDCl_3$, 500 MHz).	S-4
Figure S2.	Partial ^{1}H NMR spectrum of solidagoic acid J (**1**) ($CDCl_3$, 500 MHz) – downfield region (δ_H 6.3–4.1).	S-4
Figure S3.	Partial ^{1}H NMR spectrum of solidagoic acid J (**1**) ($CDCl_3$, 500 MHz) – aliphatic region (δ_H 2.5–0.7).	S-5
Figure S4.	^{13}C DEPTQ NMR spectrum of solidagoic acid J (**1**) ($CDCl_3$, 126 MHz).	S-5
Figure S5.	^{1}H–^{1}H COSY NMR spectrum of solidagoic acid J (**1**) ($CDCl_3$, 500 MHz).	S-6
Figure S6.	^{1}H–^{13}C edHSQC NMR spectrum of solidagoic acid J (**1**) ($CDCl_3$, 500/126 MHz).	S-6
Figure S7.	^{1}H–^{13}C band-selective HSQC NMR spectrum of solidagoic acid J (**1**) ($CDCl_3$, 500/126 MHz) – aliphatic region (δ_C 31.0–15.0).	S-7
Figure S8.	^{1}H–^{13}C HMBC NMR spectrum of solidagoic acid J (**1**) ($CDCl_3$, 500/126 MHz).	S-7
Figure S9.	^{1}H–^{13}C band-selective HMBC NMR spectrum of solidagoic acid J (**1**) ($CDCl_3$, 500/126 MHz) – aliphatic region (δ_C 21.0–15.5).	S-8
Figure S10.	^{1}H–^{13}C band-selective HMBC NMR spectrum of solidagoic acid J (**1**) ($CDCl_3$, 500/126 MHz) – double bond region (δ_C 128.2–127.5).	S-8
Figure S11.	^{1}H–^{1}H TOCSY NMR spectrum of solidagoic acid J (**1**) ($CDCl_3$, 500 MHz).	S-9
Figure S12.	^{1}H–^{1}H ROESY NMR spectrum of solidagoic acid J (**1**) ($CDCl_3$, 500 MHz).	S-9
Figure S13.	HR-ESI^{+}-MS spectrum of solidagoic acid J (**1**).	S-10
Figure S14.	HR-ESI^{+}-MS/MS of solidagoic acid J (**1**) with a normalized HCD collision energy of 40%.	S-10
Figure S15.	HR-ESI^{-}-MS spectrum of solidagoic acid J (**1**).	S-10
Figure S16.	HR-ESI^{-}-MS/MS of solidagoic acid J (**1**) with a normalized HCD collision energy of 40%.	S-11
Figure S17.	UV spectrum of solidagoic acid J (**1**) in ethanol.	S-11
Figure S18.	ATR-FTIR spectrum of solidagoic acid J (**1**).	S-12
Figure S19.	^{1}H NMR spectrum of solidagoic acid C (**2**) ($CDCl_3$, 500 MHz).	S-12
Figure S20.	^{13}C NMR spectrum of solidagoic acid C (**2**) ($CDCl_3$, 126 MHz).	S-13
Figure S21.	^{1}H–^{1}H DQF-COSY NMR spectrum of solidagoic acid C (**2**) ($CDCl_3$, 500 MHz).	S-13
Figure S22.	^{1}H–^{13}C edHSQC NMR spectrum of solidagoic acid C (**2**) ($CDCl_3$, 500/126 MHz).	S-14
Figure S23.	^{1}H–^{13}C HMBC NMR spectrum of solidagoic acid C (**2**) ($CDCl_3$, 500/126 MHz).	S-14
Figure S24.	^{1}H–^{1}H TOCSY NMR spectrum of solidagoic acid C (**2**) ($CDCl_3$, 500 MHz).	S-15
Figure S25.	^{1}H–^{1}H ROESY NMR spectrum of solidagoic acid C (**2**) ($CDCl_3$, 500 MHz).	S-15
Figure S26.	HR-ESI^{+}-MS spectrum of solidagoic acid C (**2**).	S-16
Figure S27.	HR-ESI^{+}-MS/MS of solidagoic acid C (**2**) with a normalized HCD collision energy of 40%.	S-16
Figure S28.	HR-ESI^{-}-MS spectrum of solidagoic acid C (**2**).	S-16
Figure S29.	HR-ESI^{-}-MS/MS of solidagoic acid C (**2**) with a normalized HCD collision energy of 40%.	S-17
Figure S30.	^{1}H NMR spectrum of solidagoic acid D (**3**) ($CDCl_3$, 500 MHz).	S-17

Figure S31.	^{13}C NMR spectrum of solidagoic acid D (**3**) ($CDCl_3$, 126 MHz).	S-18
Figure S32.	$^{1}H–^{1}H$ DQF-COSY NMR spectrum of solidagoic acid D (**3**) ($CDCl_3$, 500 MHz).	S-18
Figure S33.	$^{1}H–^{13}C$ edHSQC NMR spectrum of solidagoic acid D (**3**) ($CDCl_3$, 500/126 MHz).	S-19
Figure S34.	$^{1}H–^{13}C$ HMBC NMR spectrum of solidagoic acid D (**3**) ($CDCl_3$, 500/126 MHz).	S-19
Figure S35.	$^{1}H–^{1}H$ TOCSY NMR spectrum of solidagoic acid D (**3**) ($CDCl_3$, 500 MHz).	S-20
Figure S36.	$^{1}H–^{1}H$ ROESY NMR spectrum of solidagoic acid D (**3**) ($CDCl_3$, 500 MHz).	S-20
Figure S37.	HR-ESI^+-MS spectrum of solidagoic acid D (**3**).	S-21
Figure S38.	HR-ESI^+-MS/MS of solidagoic acid D (**3**) with a normalized HCD collision energy of 20%.	S-21
Figure S39.	HR-ESI^--MS spectrum of solidagoic acid D (**3**).	S-21
Figure S40.	HR-ESI^--MS/MS of solidagoic acid D (**3**) with a normalized HCD collision energy of 50%.	S-22
Figure S41.	^{1}H NMR spectrum of 1-linoleoyl glycerol (**4**) ($CDCl_3$, 500 MHz).	S-22
Figure S42.	^{13}C NMR spectrum of 1-linoleoyl glycerol (**4**) ($CDCl_3$, 126 MHz).	S-23
Figure S43.	$^{1}H–^{1}H$ DQF-COSY NMR spectrum of 1-linoleoyl glycerol (**4**) ($CDCl_3$, 500 MHz).	S-23
Figure S44.	$^{1}H–^{13}C$ edHSQC NMR spectrum of 1-linoleoyl glycerol (**4**) ($CDCl_3$, 500/126 MHz).	S-24
Figure S45.	$^{1}H–^{13}C$ HMBC NMR spectrum of 1-linoleoyl glycerol (**4**) ($CDCl_3$, 500/126 MHz).	S-24
Figure S46.	$^{1}H–^{1}H$ TOCSY NMR spectrum of 1-linoleoyl glycerol (**4**) ($CDCl_3$, 500 MHz).	S-25
Figure S47.	HR-ESI^+-MS spectrum of 1-linoleoyl glycerol (**4**).	S-25
Figure S48.	HR-ESI^+-MS/MS of 1-linoleoyl glycerol (**4**) with a normalized HCD collision energy of 50%.	S-26
Figure S49.	^{1}H NMR spectrum of 1-α-linolenoyl glycerol (**5**) ($CDCl_3$, 500 MHz).	S-26
Figure S50.	^{13}C NMR spectrum of 1-α-linolenoyl glycerol (**5**) ($CDCl_3$, 126 MHz).	S-27
Figure S51.	$^{1}H–^{1}H$ DQF-COSY NMR spectrum of 1-α-linolenoyl glycerol (**5**) ($CDCl_3$, 500 MHz).	S-27
Figure S52.	$^{1}H–^{13}C$ edHSQC NMR spectrum of 1-α-linolenoyl glycerol (**5**) ($CDCl_3$, 500/126 MHz).	S-28
Figure S53.	$^{1}H–^{13}C$ HMBC NMR spectrum of 1-α-linolenoyl glycerol (**5**) ($CDCl_3$, 500/126 MHz).	S-28
Figure S54.	$^{1}H–^{1}H$ TOCSY NMR spectrum of 1-α-linolenoyl glycerol (**5**) ($CDCl_3$, 500 MHz).	S-29
Figure S55.	HR-ESI^+-MS spectrum of 1-α-linolenoyl glycerol (**5**).	S-29
Figure S56.	HR-ESI^+-MS/MS of 1-α-linolenoyl glycerol (**5**) with a normalized HCD collision energy of 50%.	S-30

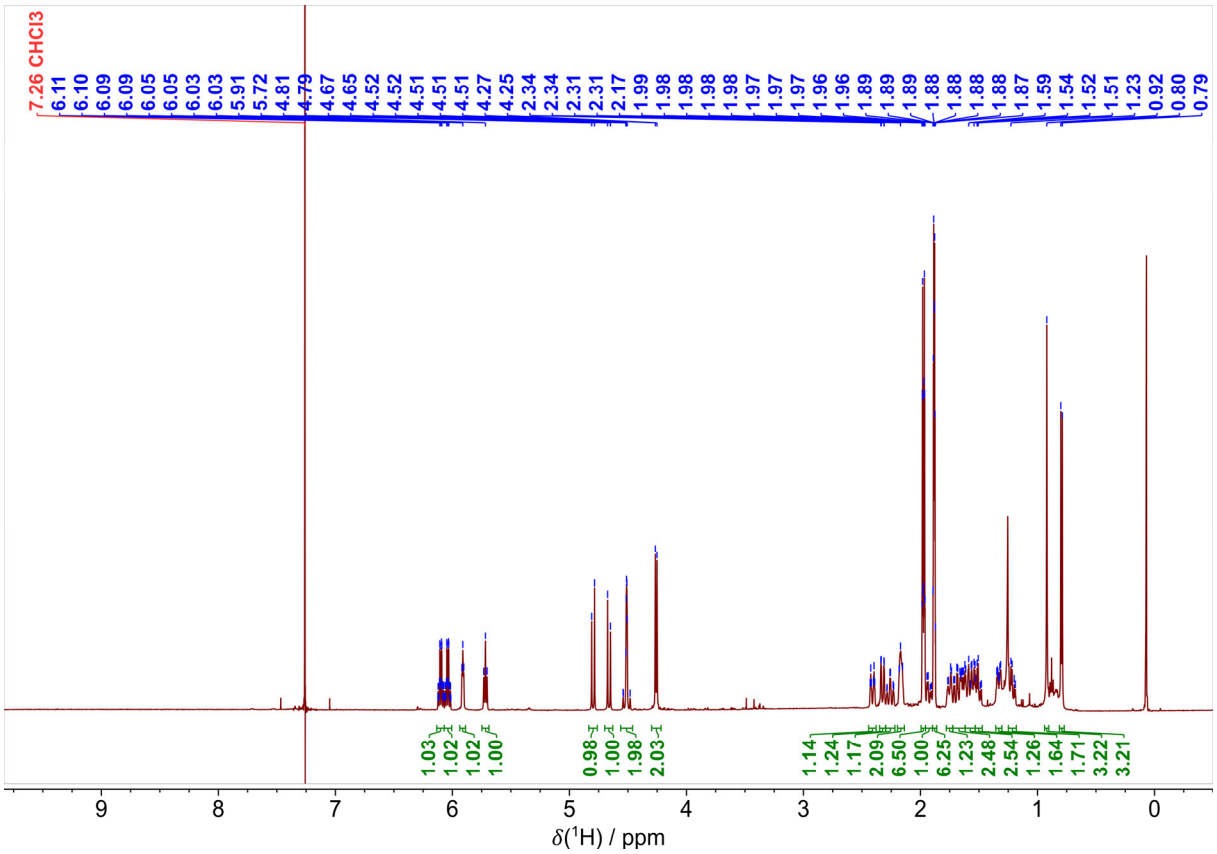


Figure S1. ^{1}H NMR spectrum of solidagoic acid J (**1**) ($CDCl_3$, 500 MHz).

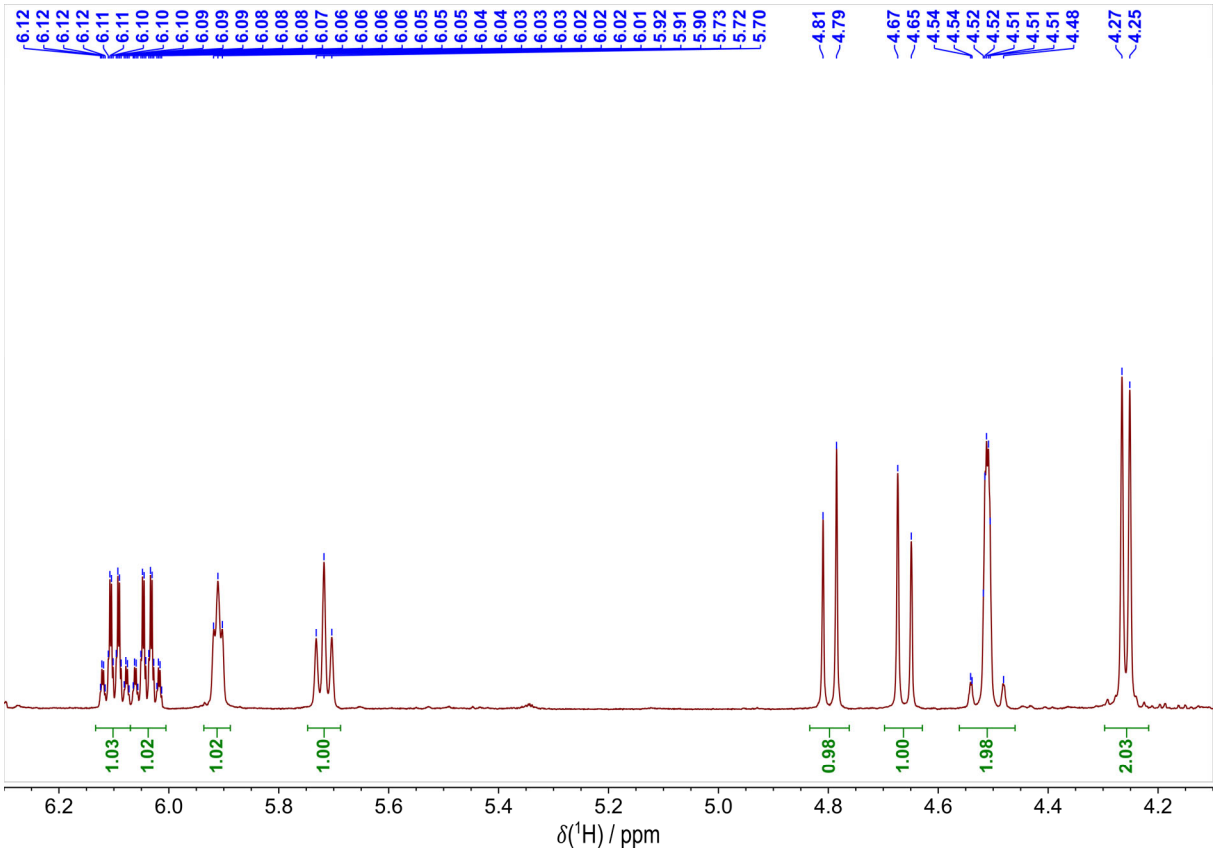


Figure S2. Partial ^{1}H NMR spectrum of solidagoic acid J (**1**) ($CDCl_3$, 500 MHz) – downfield region (δ_H 6.3–4.1).

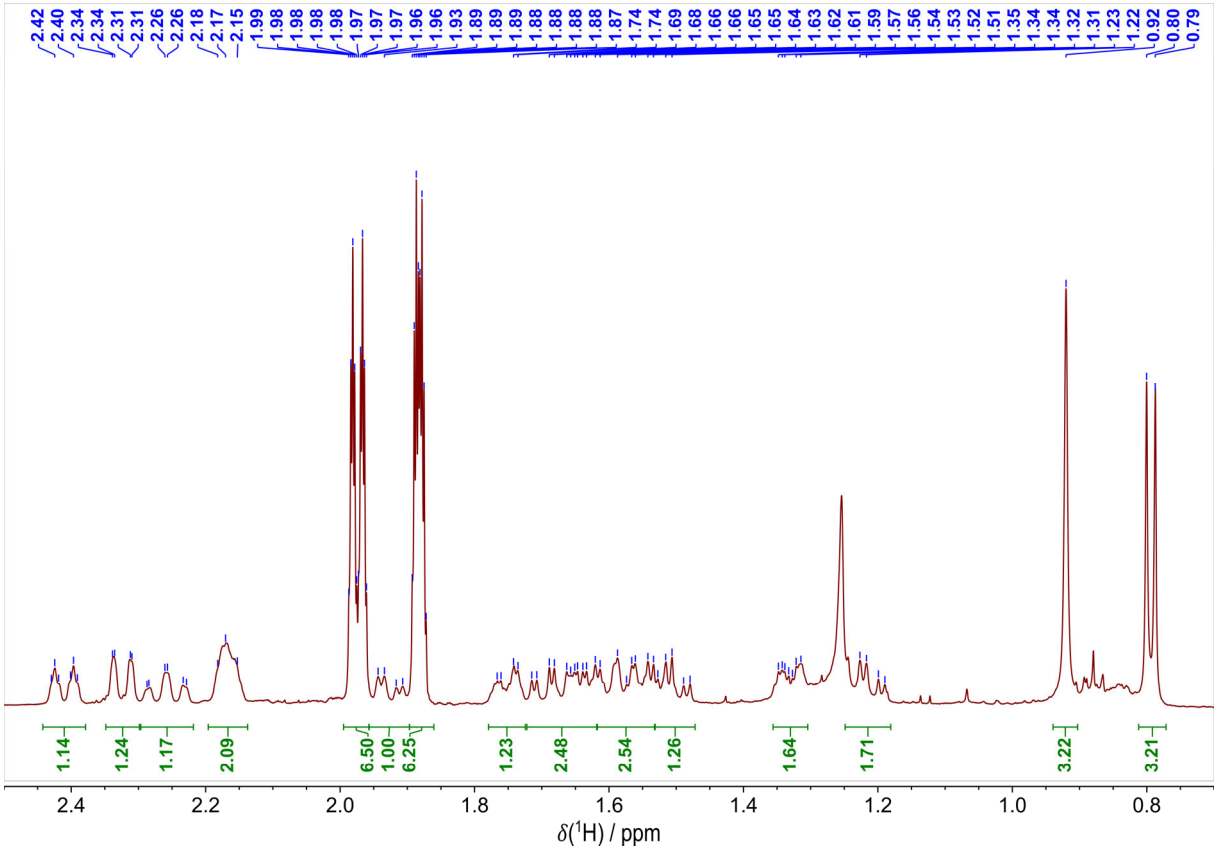


Figure S3. Partial ^{1}H NMR spectrum of solidagoic acid J (**1**) ($CDCl_3$, 500 MHz) – aliphatic region (δ_H 2.5–0.7).

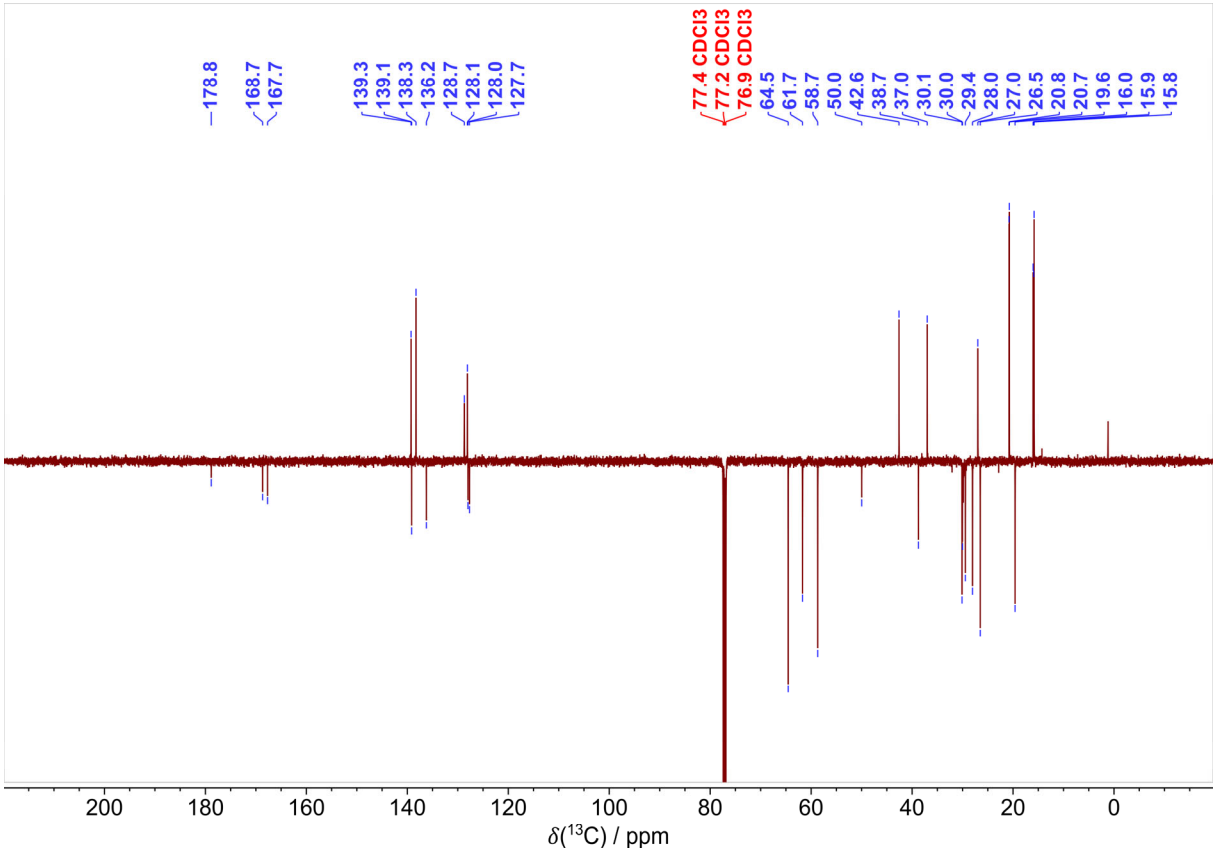


Figure S4. ^{13}C DEPTQ NMR spectrum of solidagoic acid J (**1**) ($CDCl_3$, 126 MHz).

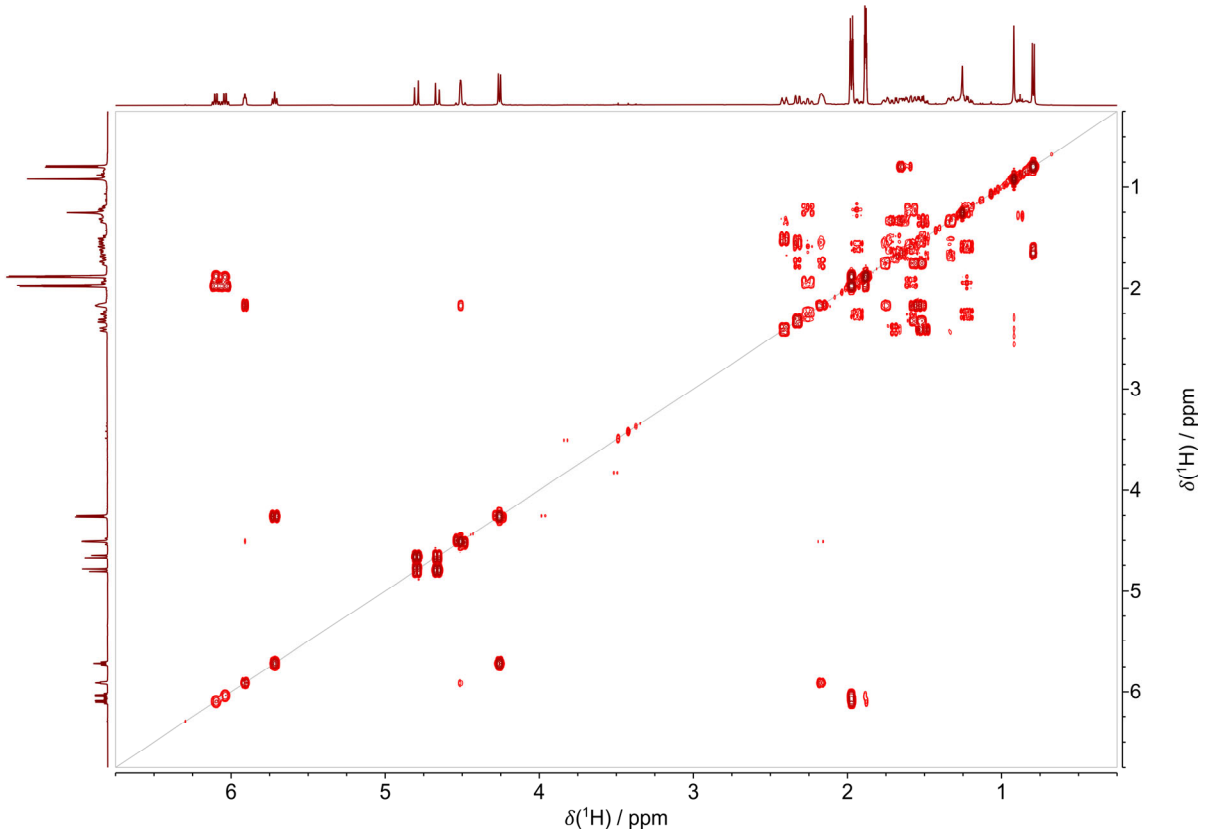


Figure S5. ^{1}H–^{1}H COSY NMR spectrum of solidagoic acid J (**1**) ($CDCl_3$, 500 MHz).

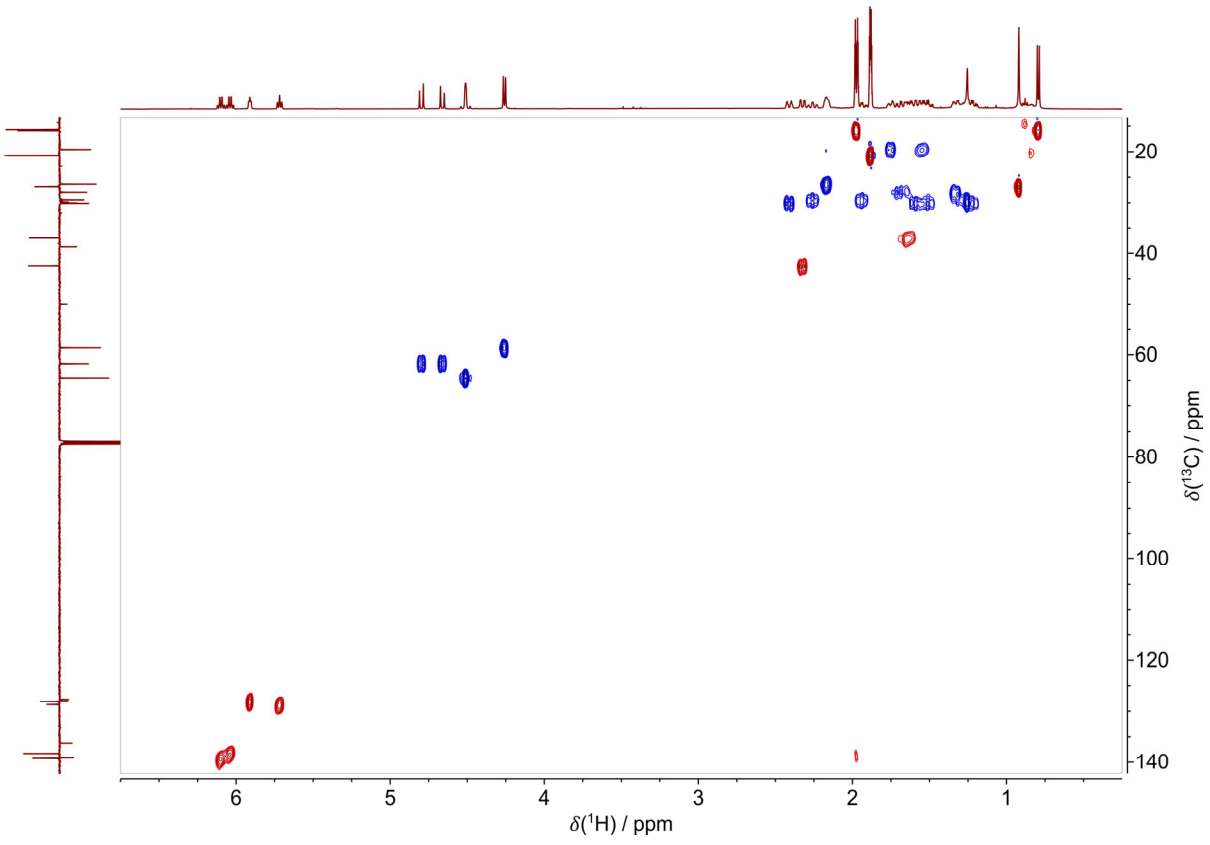


Figure S6. ^{1}H–^{13}C edHSQC NMR spectrum of solidagoic acid J (**1**) ($CDCl_3$, 500/126 MHz).

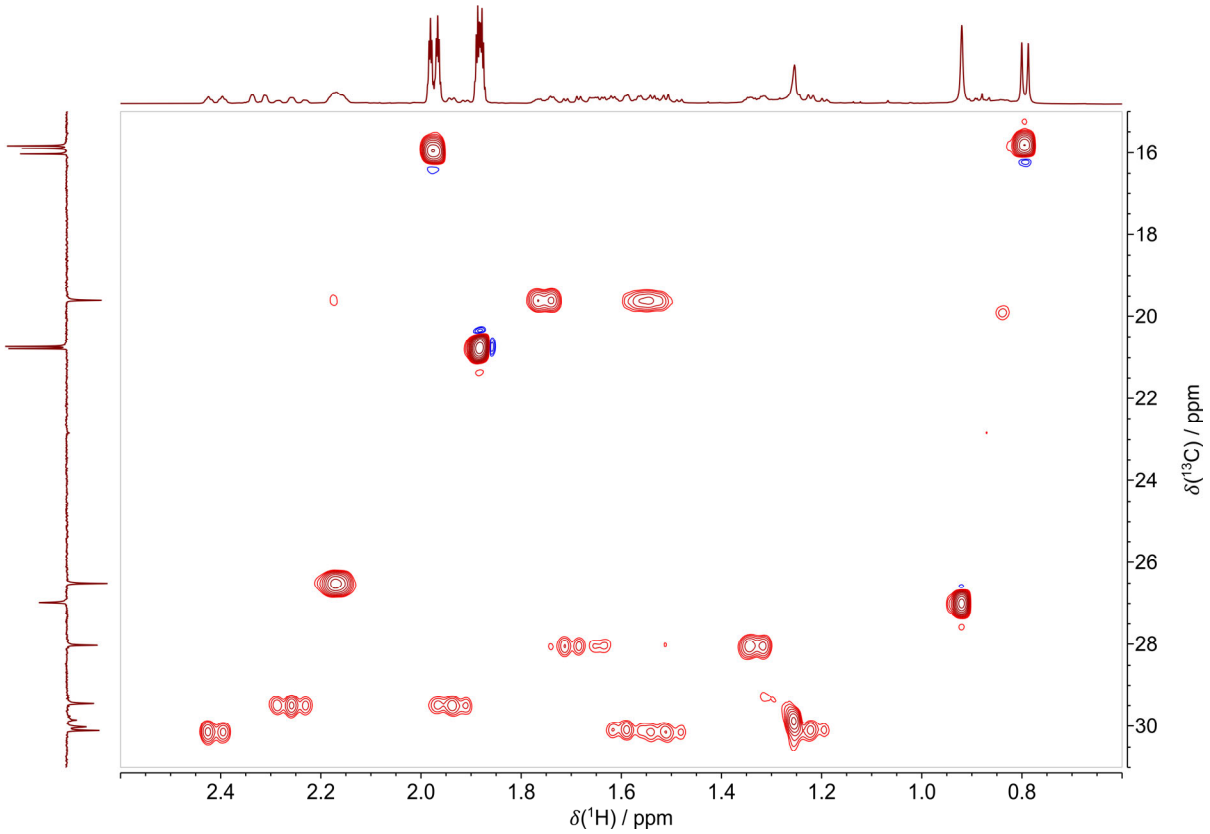


Figure S7. $^{1}H–^{13}C$ band-selective HSQC NMR spectrum of solidagoic acid J (**1**) ($CDCl_3$, 500/126 MHz) – aliphatic region (δ_C 31.0–15.0).

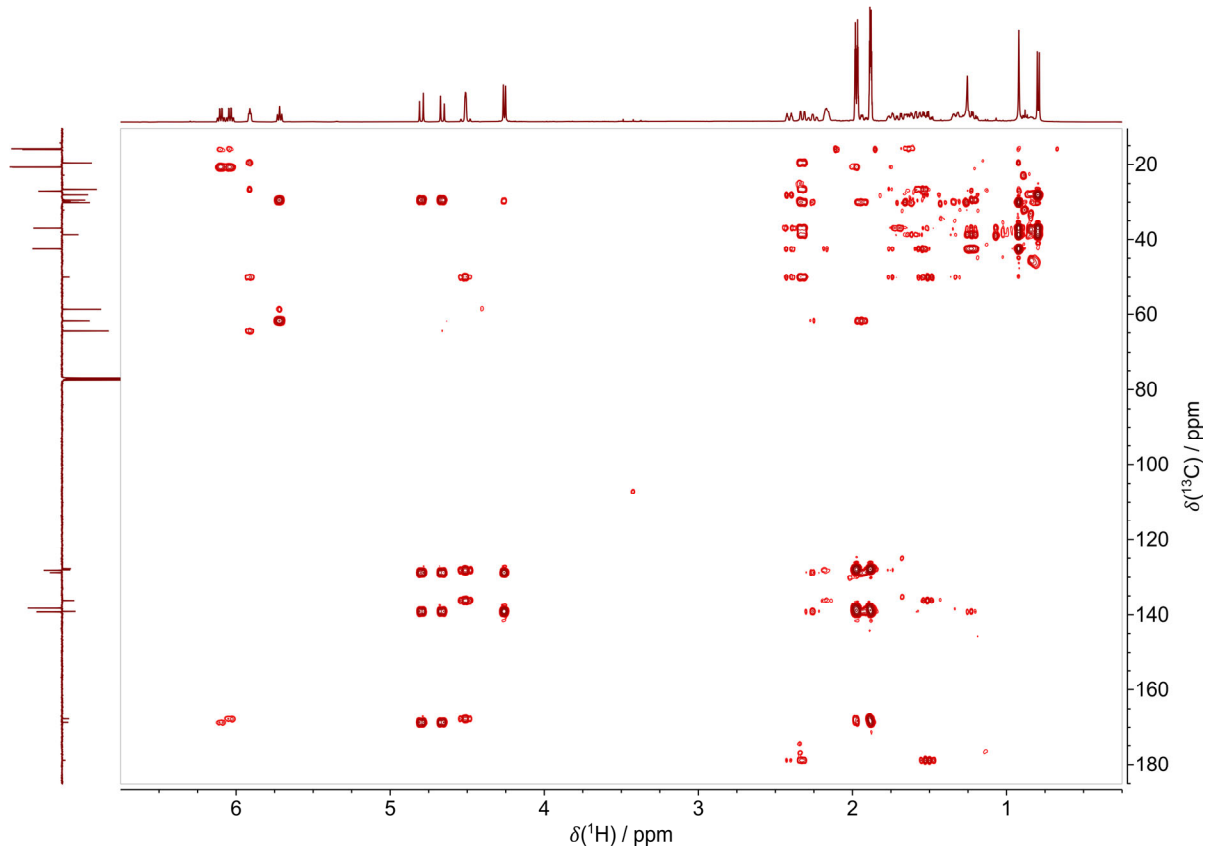


Figure S8. $^{1}H–^{13}C$ HMBC NMR spectrum of solidagoic acid J (**1**) ($CDCl_3$, 500/126 MHz).

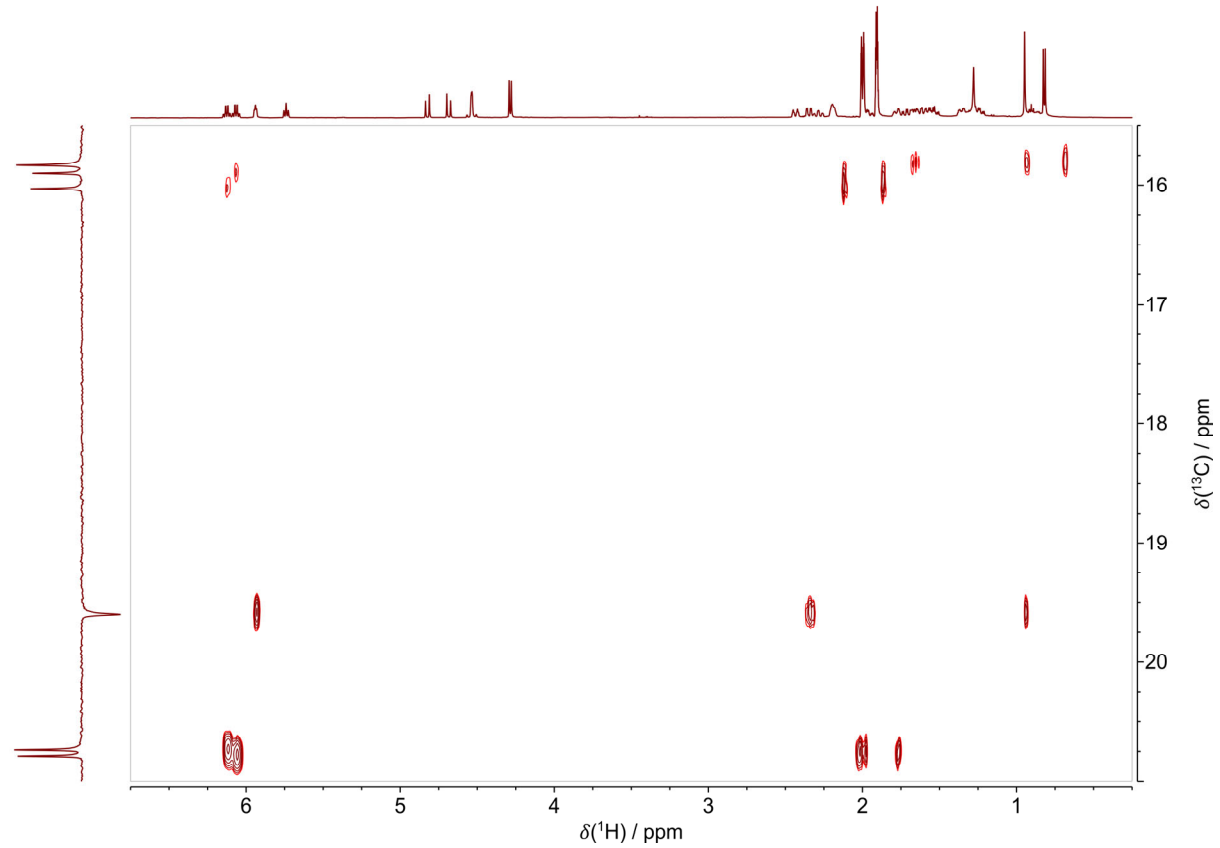


Figure S9. $^{1}H–^{13}C$ band-selective HMBC NMR spectrum of solidagoic acid J (**1**) ($CDCl_3$, 500/126 MHz) – aliphatic region (δ_C 21.0–15.5).

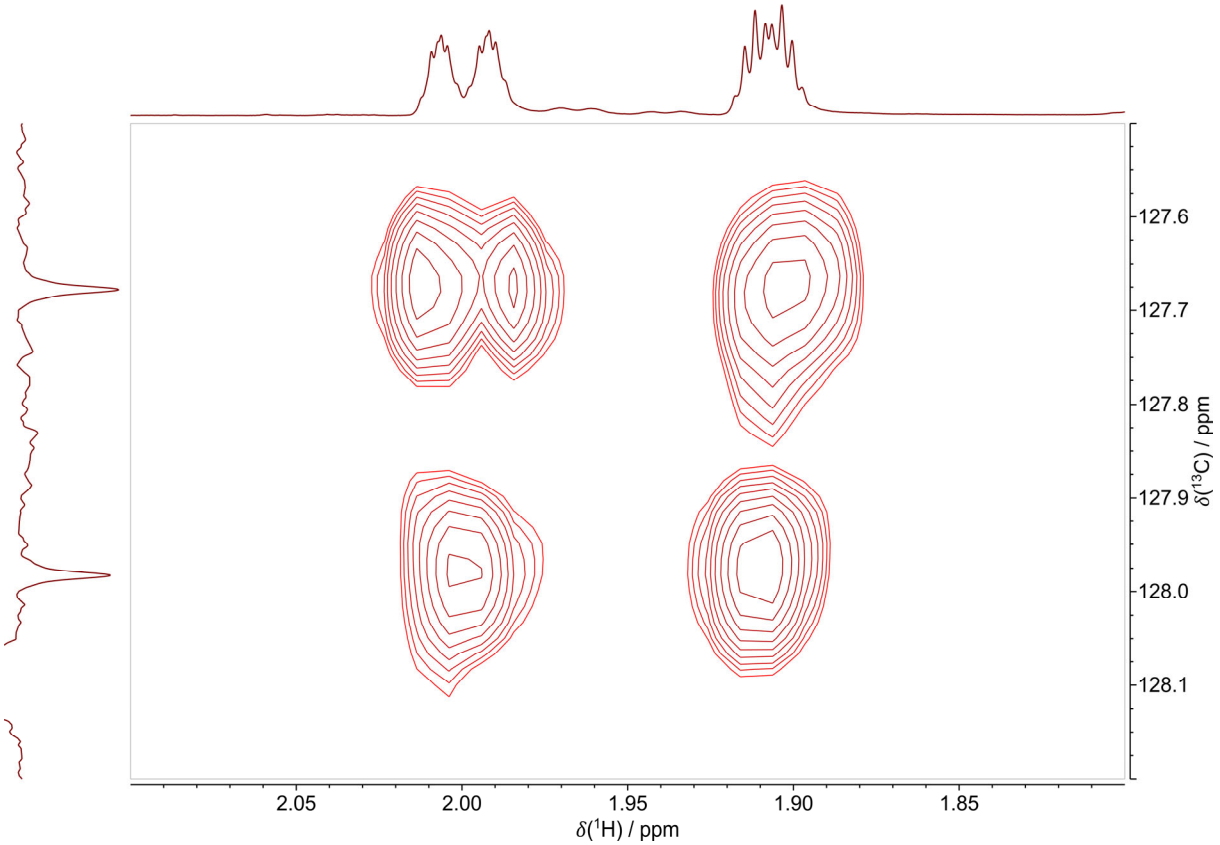


Figure S10. $^{1}H–^{13}C$ band-selective HMBC NMR spectrum of solidagoic acid J (**1**) ($CDCl_3$, 500/126 MHz) – double bond region (δ_C 128.2–127.5).

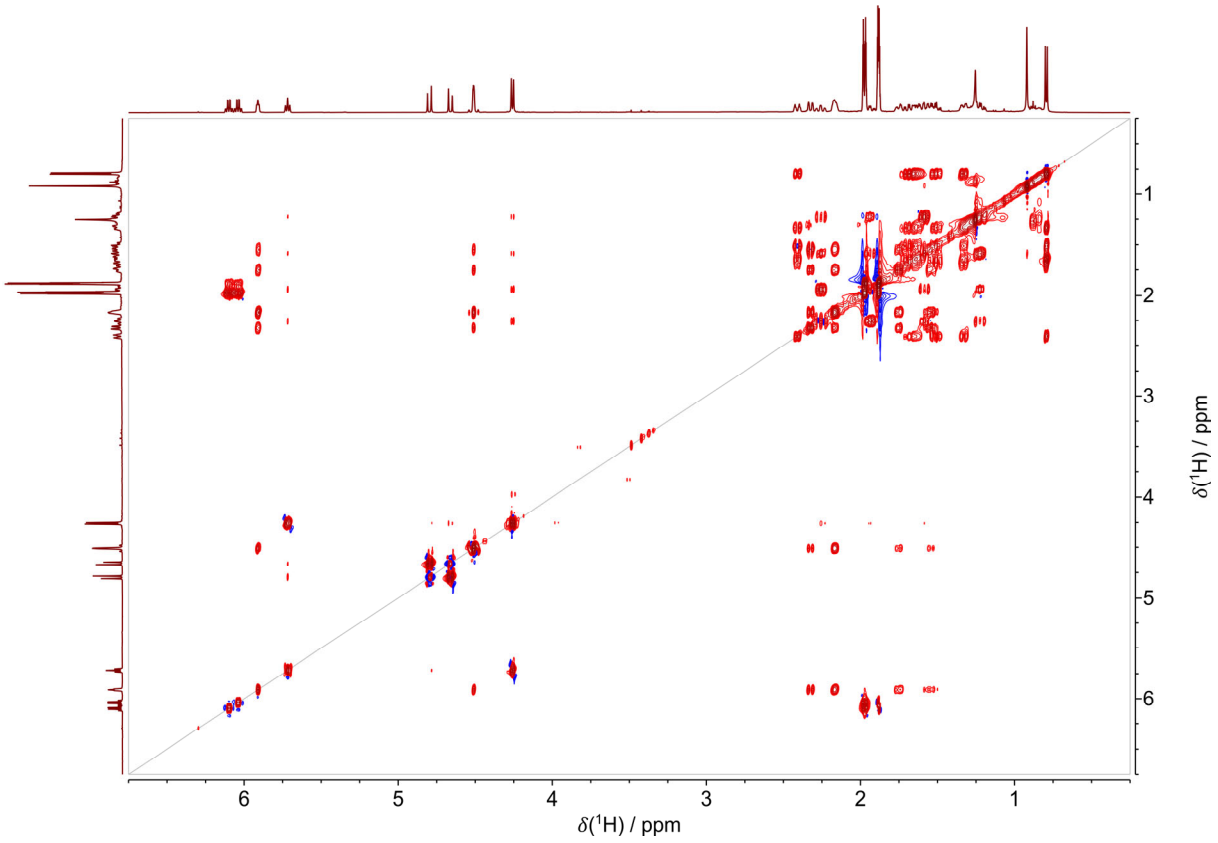


Figure S11. ^{1}H–^{1}H TOCSY NMR spectrum of solidagoic acid J (**1**) ($CDCl_3$, 500 MHz).

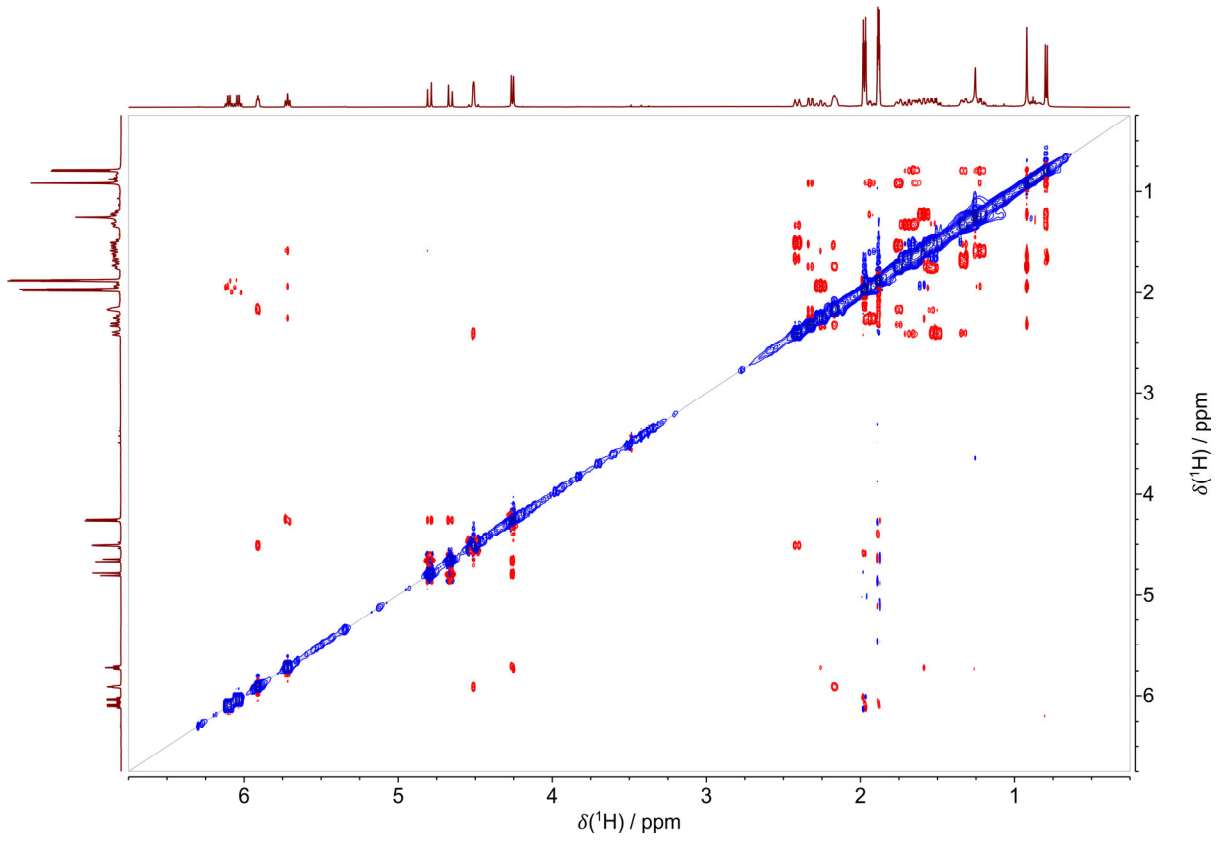


Figure S12. ^{1}H–^{1}H ROESY NMR spectrum of solidagoic acid J (**1**) ($CDCl_3$, 500 MHz).

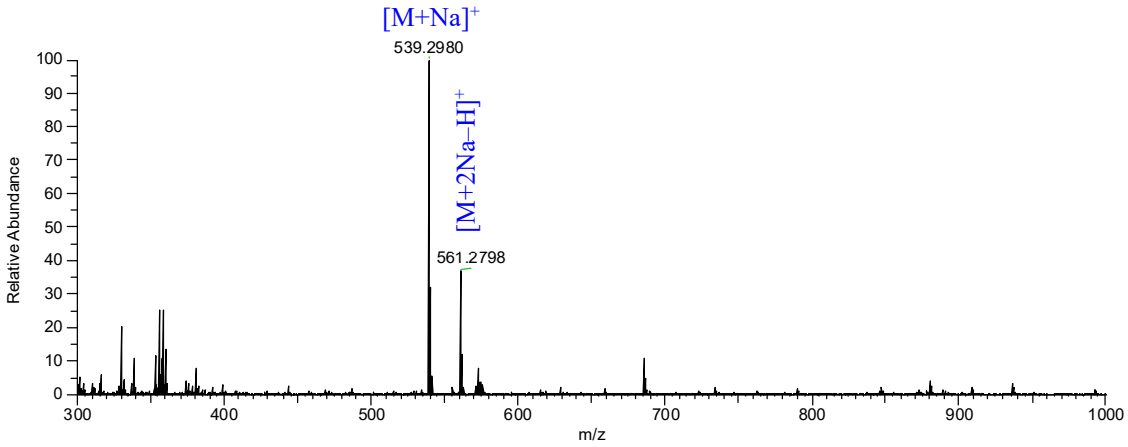


Figure S13. HR-ESI$^+$-MS spectrum of solidagoic acid J (**1**), *m*/*z* 539.2980 [M+Na]$^+$ (calculated for $C_{30}H_{44}O_7Na^+$, *m*/*z* 539.2979 [M+Na]$^+$, error: 0.1 ppm).

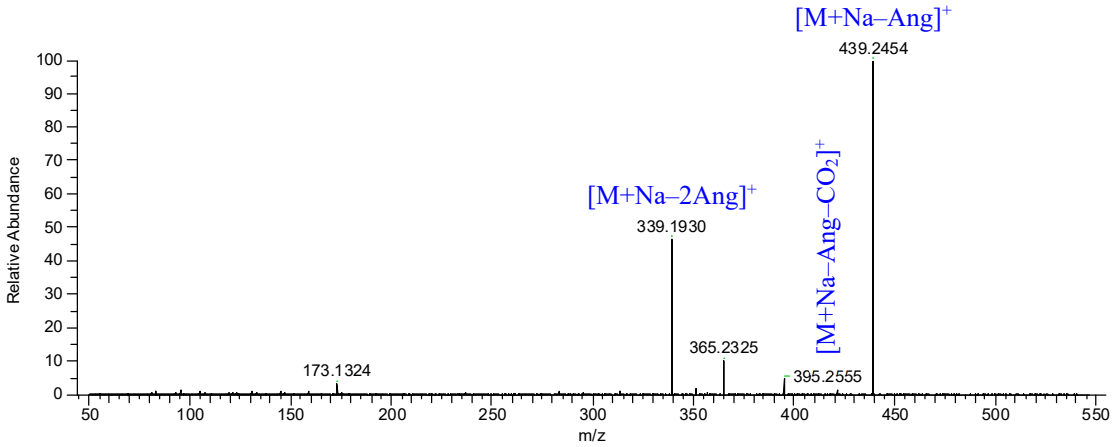


Figure S14. HR-ESI$^+$-MS/MS of solidagoic acid J (**1**) with a normalized HCD collision energy of 40%. Precursor ion: *m*/*z* 539.2979 [M+Na]$^+$, $C_{30}H_{44}O_7Na^+$. Ang denotes an angelate group ($C_5H_8O_2$).

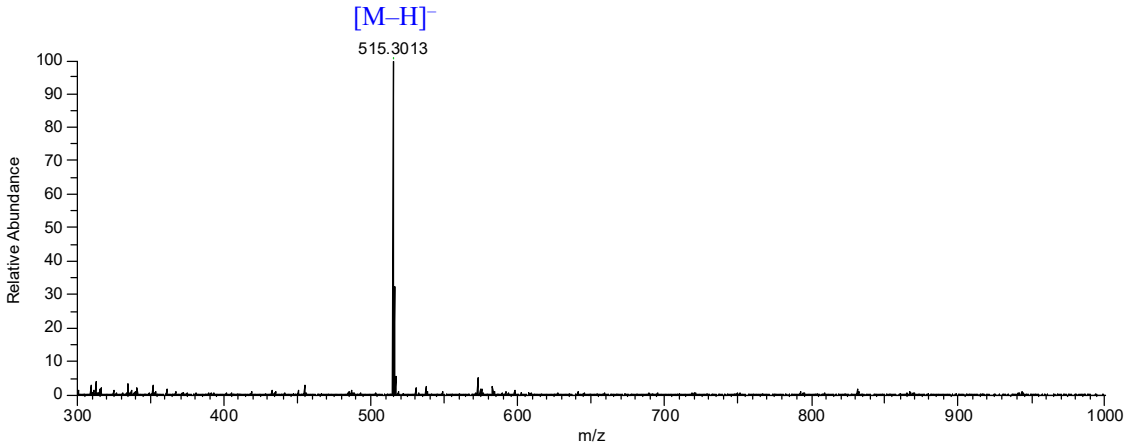


Figure S15. HR-ESI$^-$-MS spectrum of solidagoic acid J (**1**), *m*/*z* 515.3013 [M–H]$^-$ (calculated for $C_{30}H_{43}O_7^-$, *m*/*z* 515.3014 [M–H]$^-$, error: –0.3 ppm).

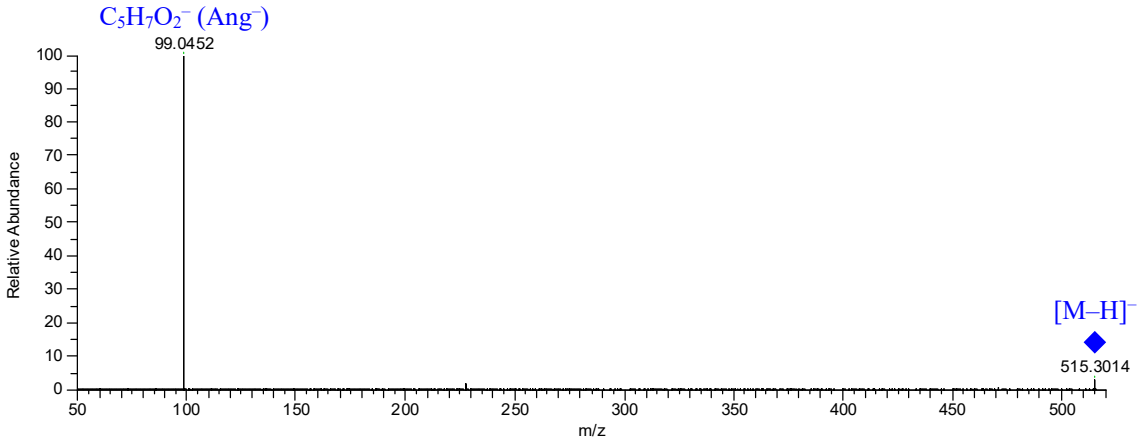


Figure S16. HR-ESI$^-$-MS/MS of solidagoic acid J (**1**) with a normalized HCD collision energy of 40%.

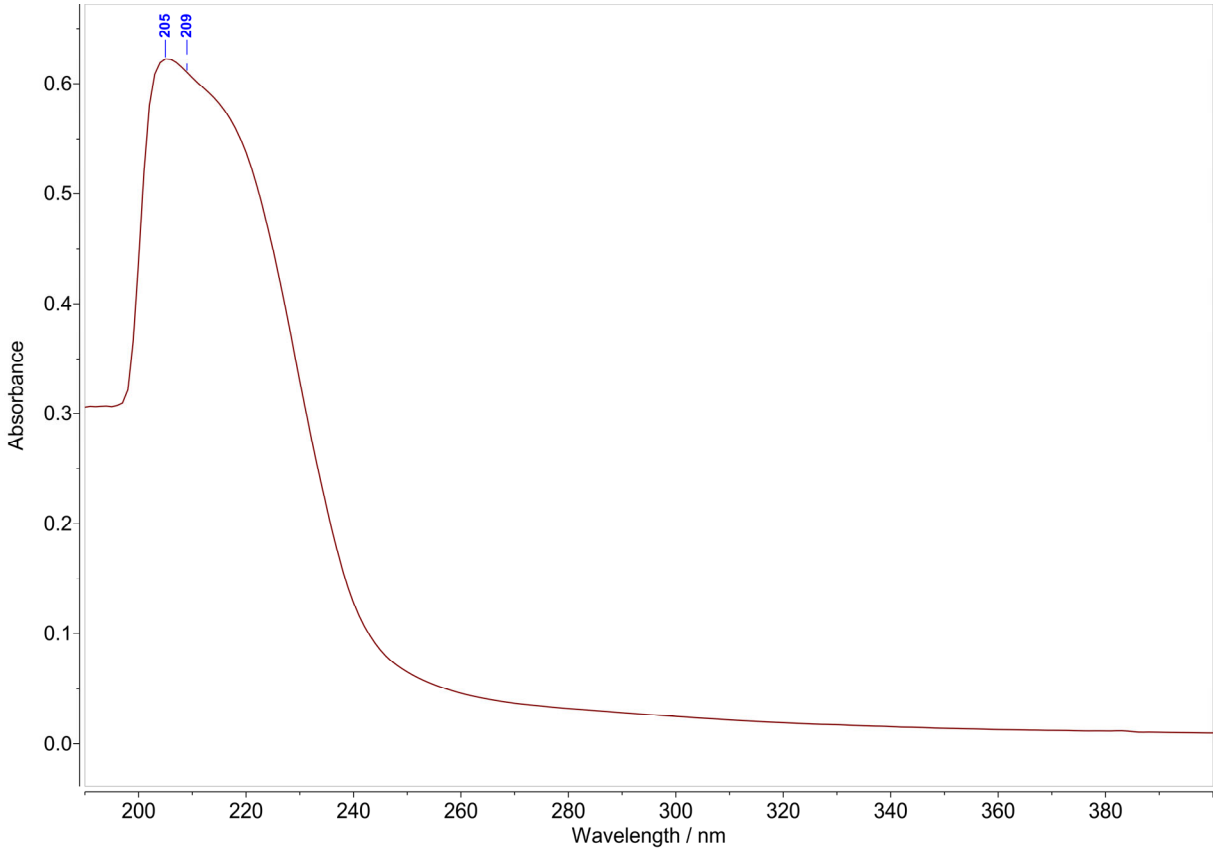


Figure S17. UV spectrum of solidagoic acid J (**1**) in ethanol.

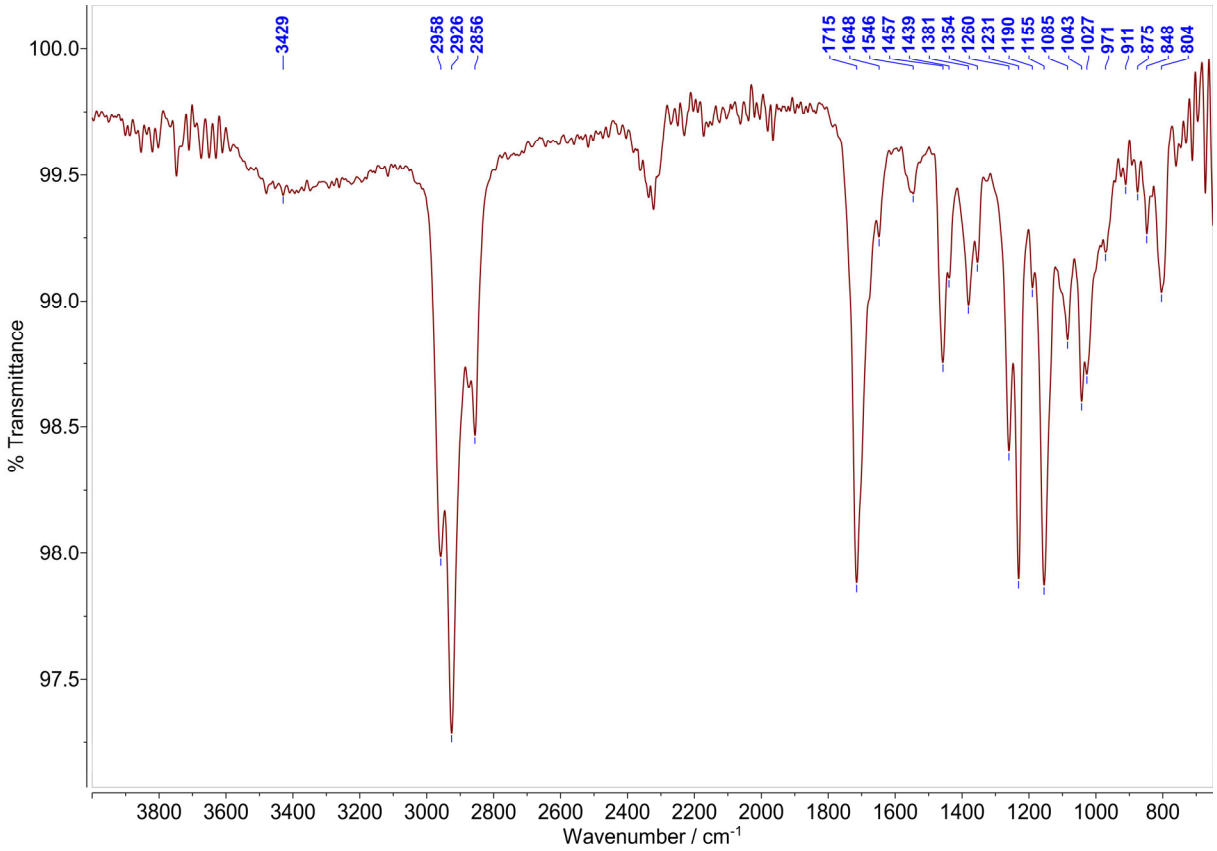


Figure S18. ATR-FTIR spectrum of solidagoic acid J (**1**).

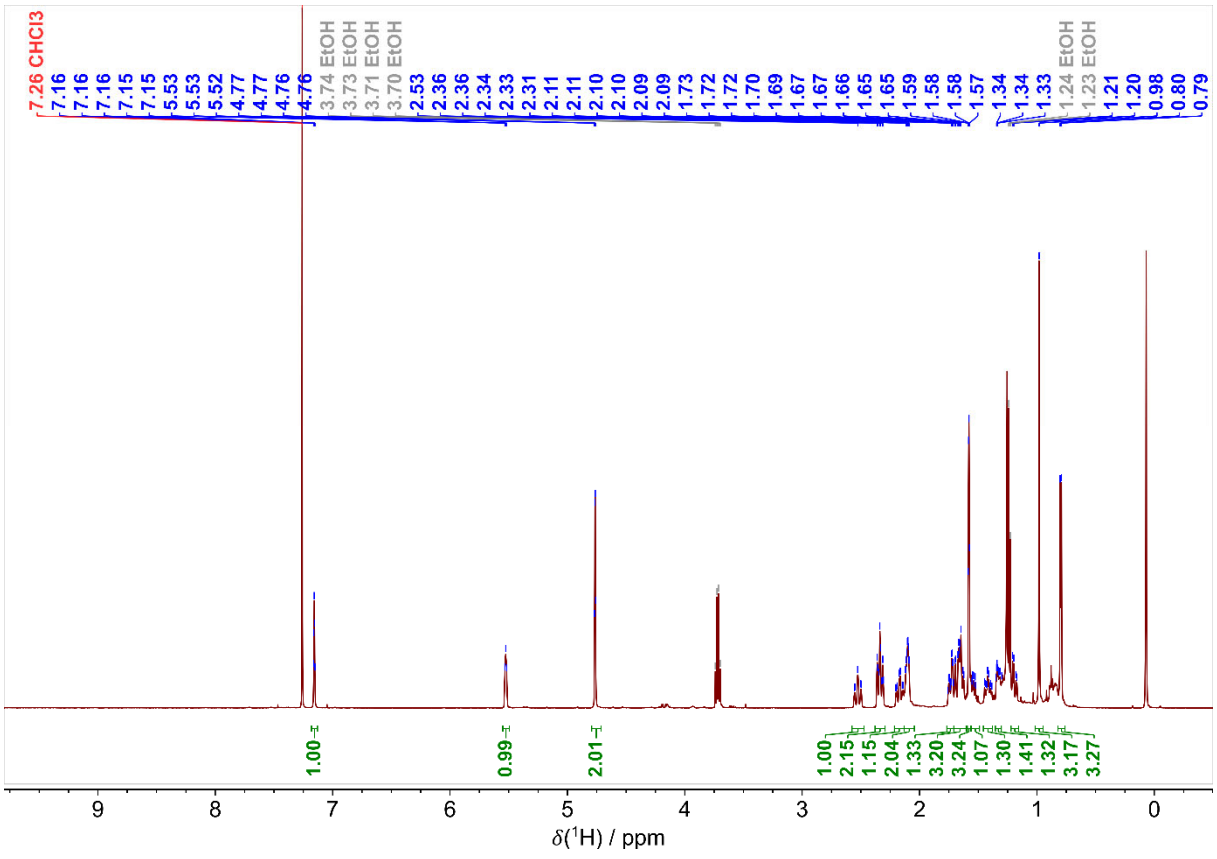


Figure S19. ^{1}H NMR spectrum of solidagoic acid C (**2**) ($CDCl_3$, 500 MHz).

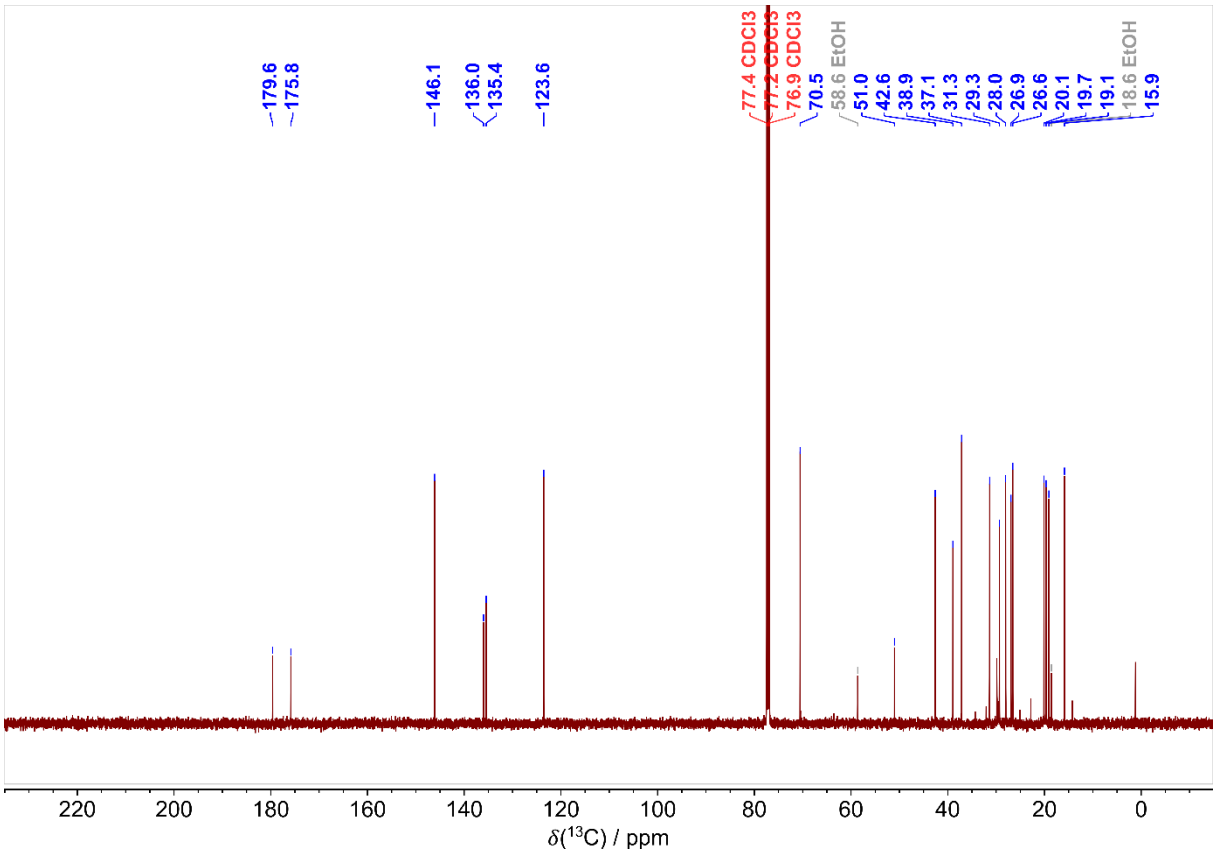


Figure S20. ^{13}C NMR spectrum of solidagoic acid C (**2**) ($CDCl_3$, 126 MHz).

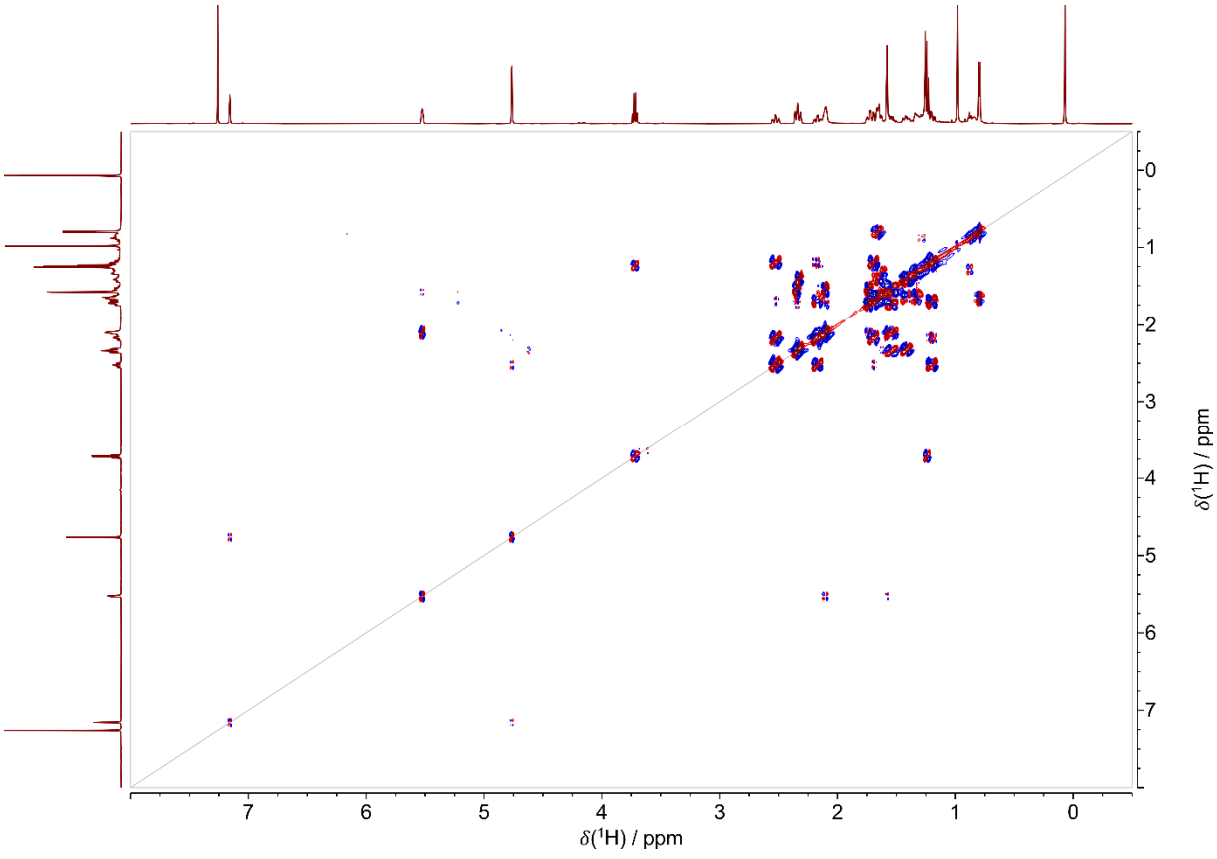


Figure S21. ^{1}H–^{1}H DQF-COSY NMR spectrum of solidagoic acid C (**2**) ($CDCl_3$, 500 MHz).

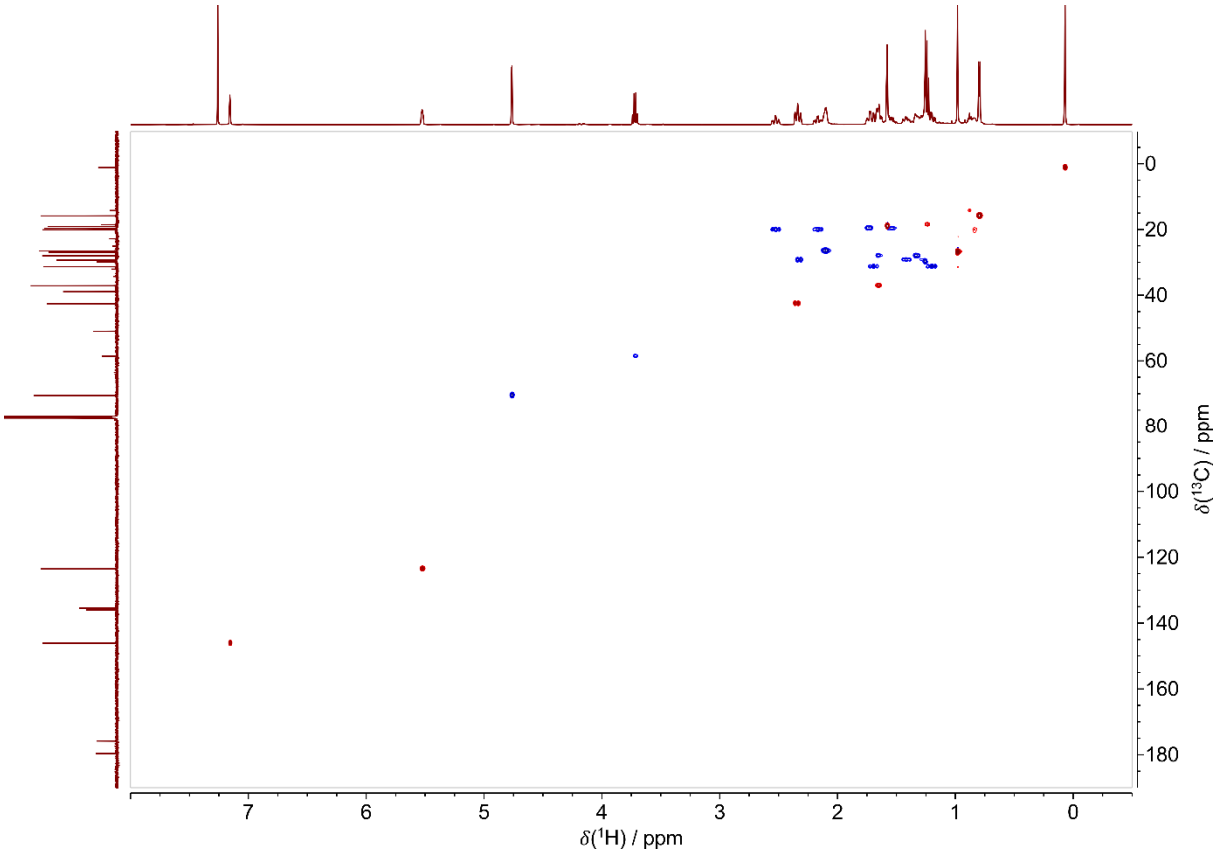


Figure S22. $^{1}H–^{13}C$ edHSQC NMR spectrum of solidagoic acid C (**2**) ($CDCl_3$, 500/126 MHz).

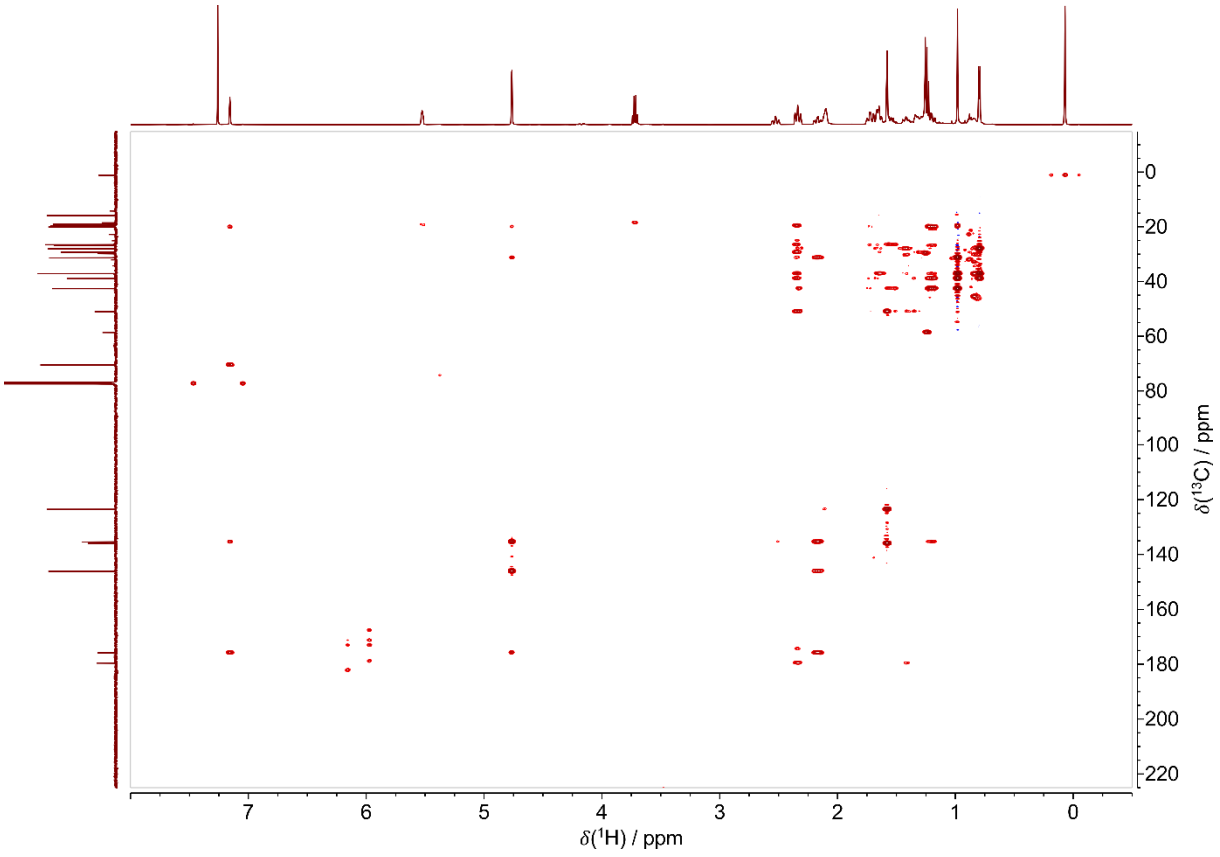


Figure S23. $^{1}H–^{13}C$ HMBC NMR spectrum of solidagoic acid C (**2**) ($CDCl_3$, 500/126 MHz).

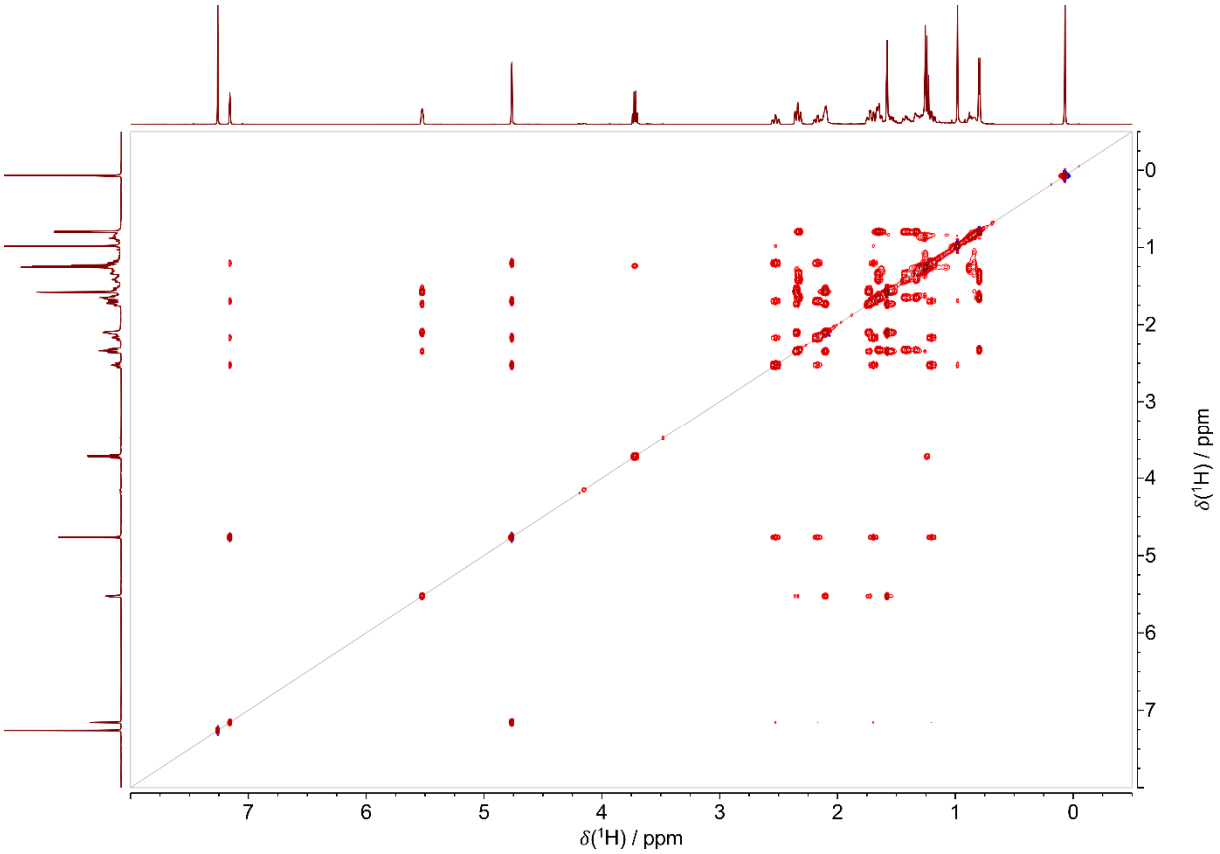


Figure S24. ^{1}H–^{1}H TOCSY NMR spectrum of solidagoic acid C (**2**) ($CDCl_3$, 500 MHz).

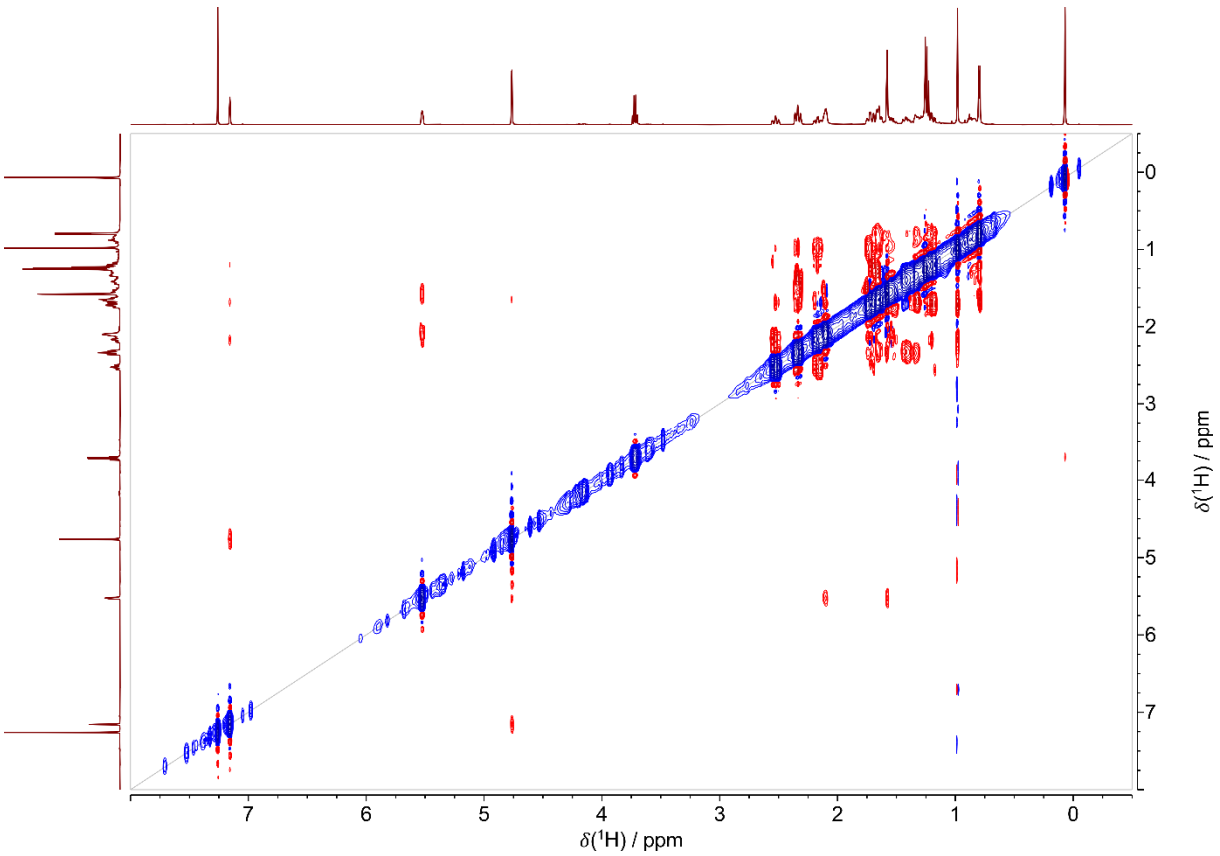


Figure S25. ^{1}H–^{1}H ROESY NMR spectrum of solidagoic acid C (**2**) ($CDCl_3$, 500 MHz).

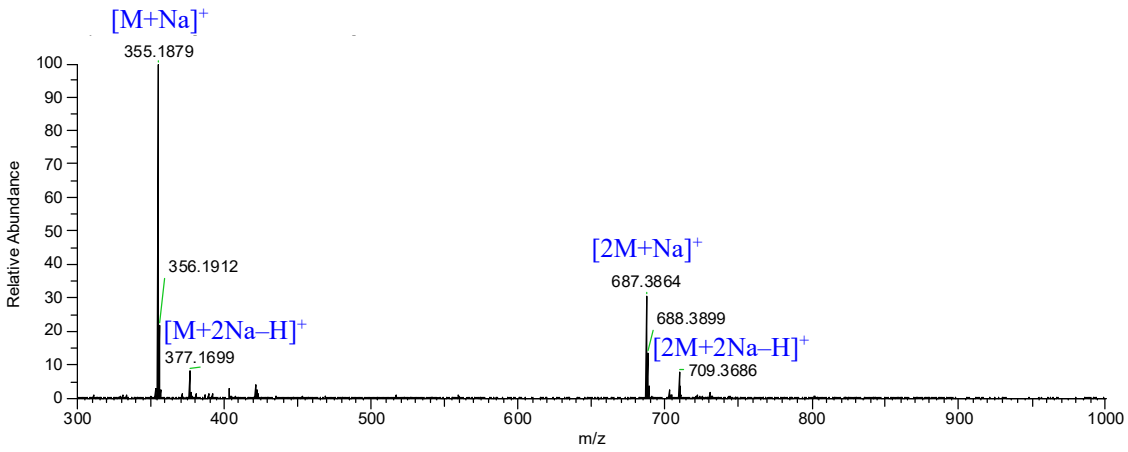


Figure S26. HR-ESI$^+$-MS spectrum of solidagoic acid C (**2**), *m/z* 355.1879 $[M+Na]^+$ (calculated for $C_{20}H_{28}O_4Na^+$, *m/z* 355.1880 $[M+Na]^+$, error: –0.1 ppm).

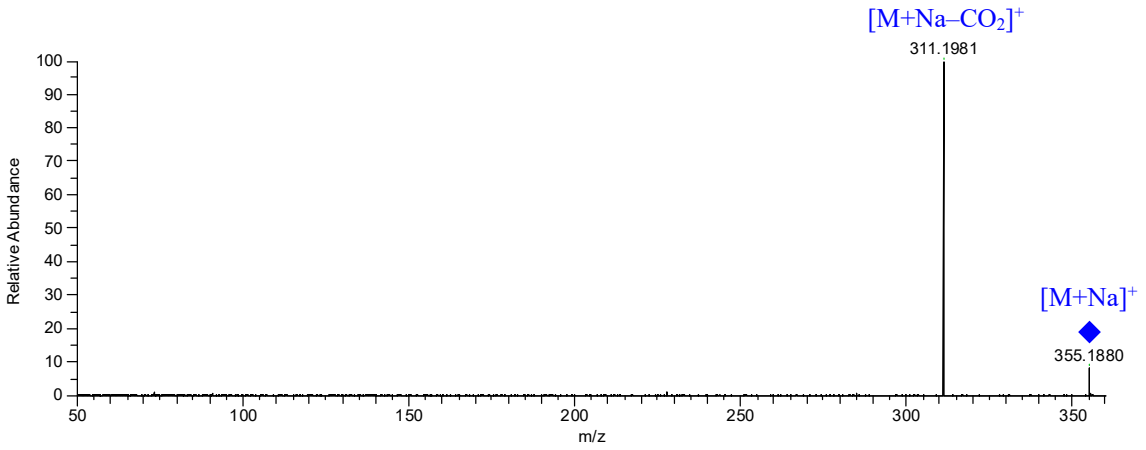


Figure S27. HR-ESI$^+$-MS/MS of solidagoic acid C (**2**) with a normalized HCD collision energy of 40%. Precursor ion: *m/z* 355.1880 $[M+Na]^+$, $C_{20}H_{28}O_4Na^+$.

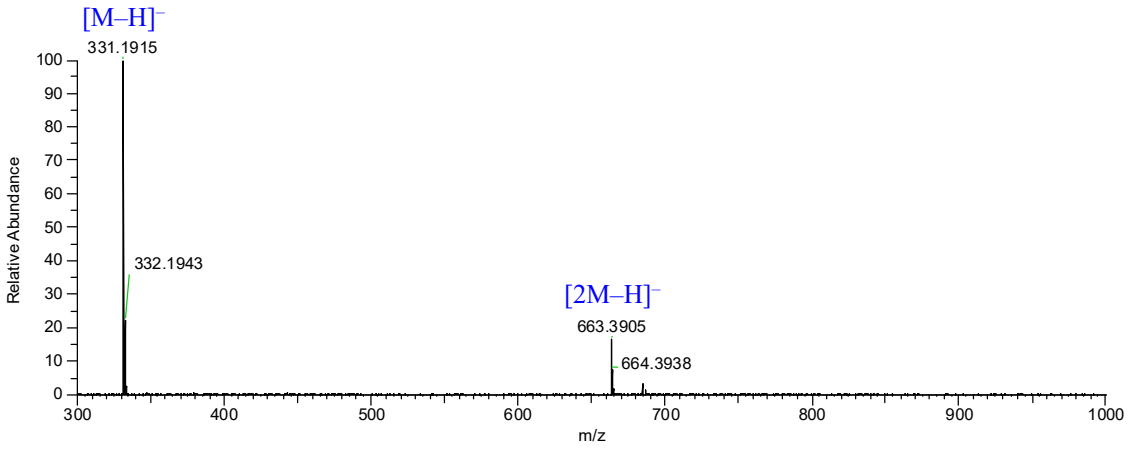


Figure S28. HR-ESI$^-$-MS spectrum of solidagoic acid C (**2**), *m/z* 331.1915 $[M–H]^-$ (calculated for $C_{20}H_{27}O_4^-$, *m/z* 331.1915 $[M–H]^-$, error: –0.1 ppm).

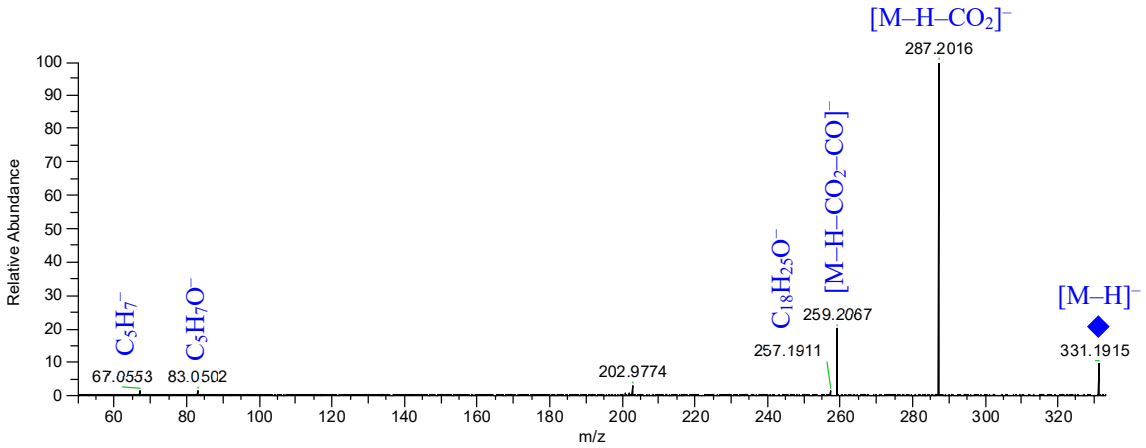


Figure S29. HR-ESI$^-$-MS/MS of solidagoic acid C (**2**) with a normalized HCD collision energy of 40%. Precursor ion: *m*/*z* 331.1915 $[M–H]^-$, $C_{20}H_{27}O_4^-$.

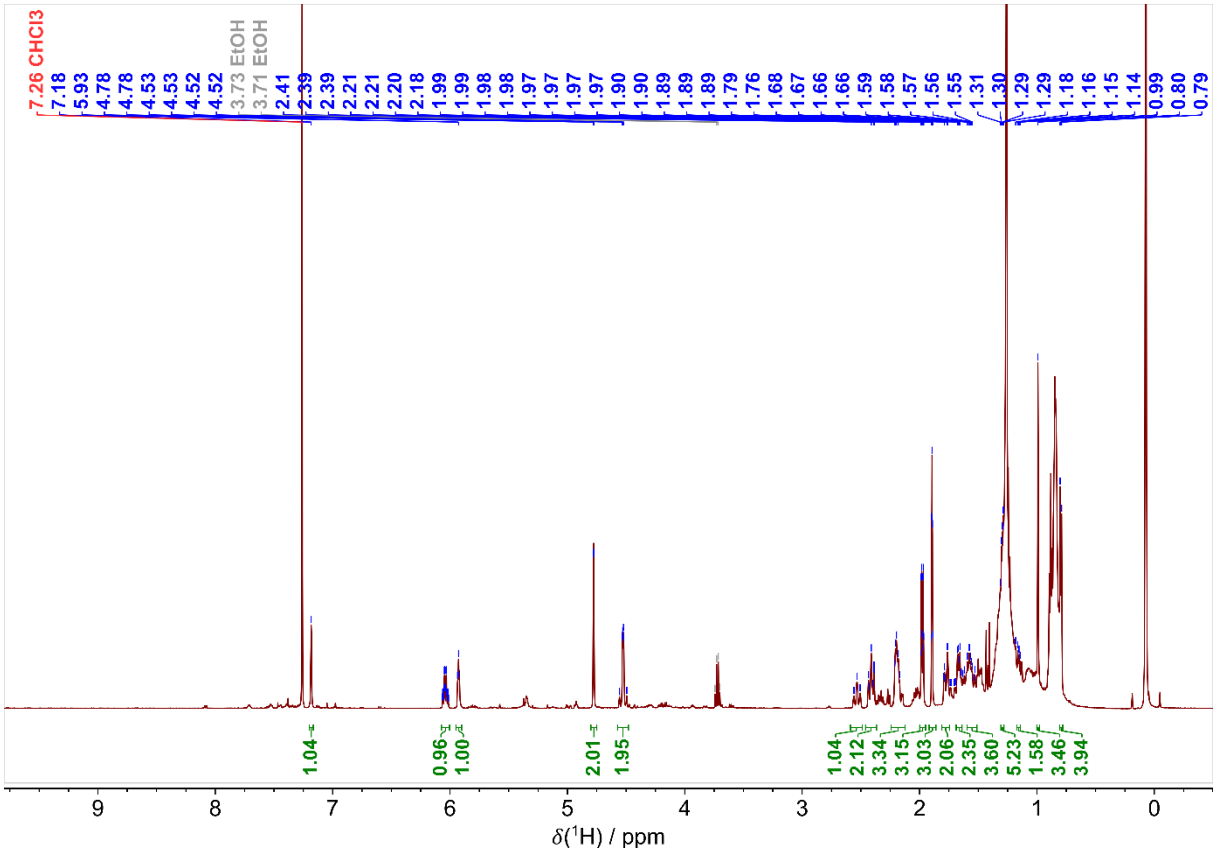


Figure S30. ^{1}H NMR spectrum of solidagoic acid D (**3**) ($CDCl_3$, 500 MHz).

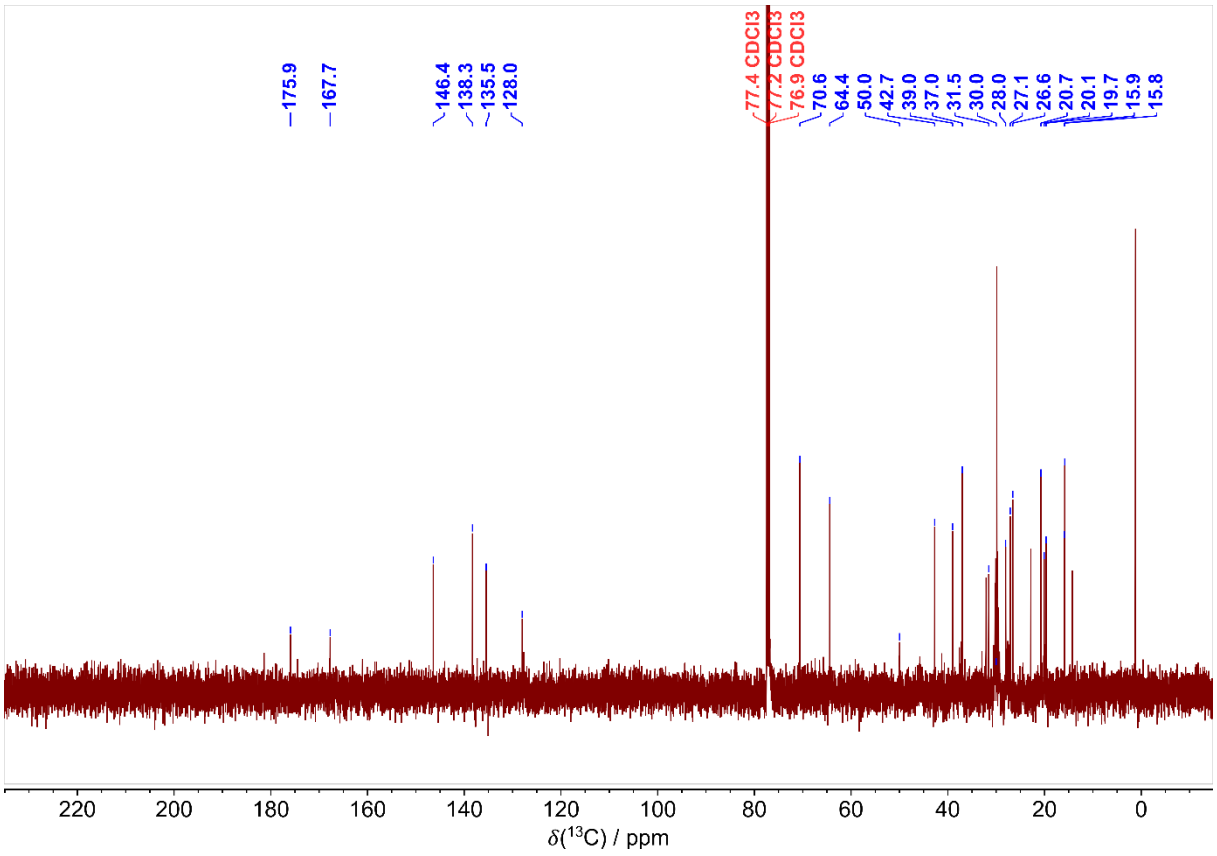


Figure S31. ^{13}C NMR spectrum of solidagoic acid D (**3**) ($CDCl_3$, 126 MHz).

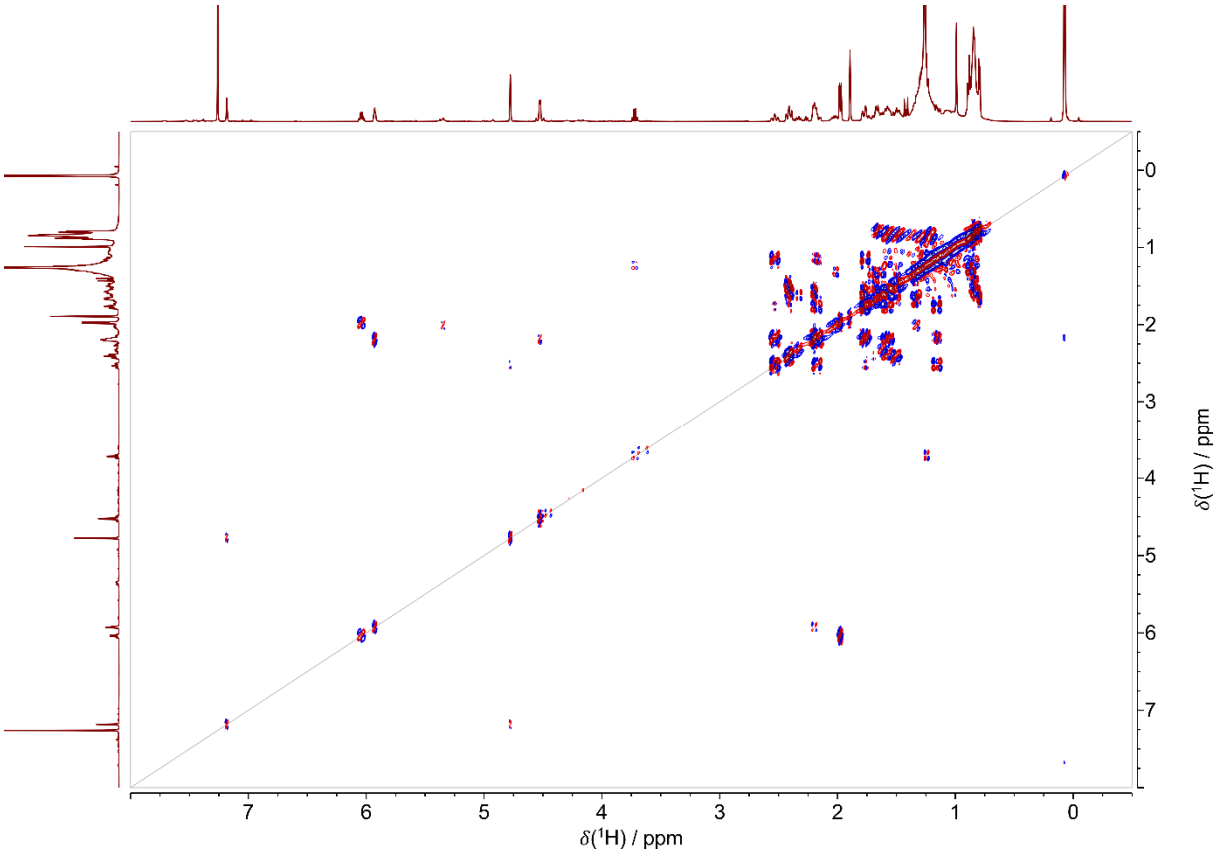


Figure S32. ^{1}H–^{1}H DQF-COSY NMR spectrum of solidagoic acid D (**3**) ($CDCl_3$, 500 MHz).

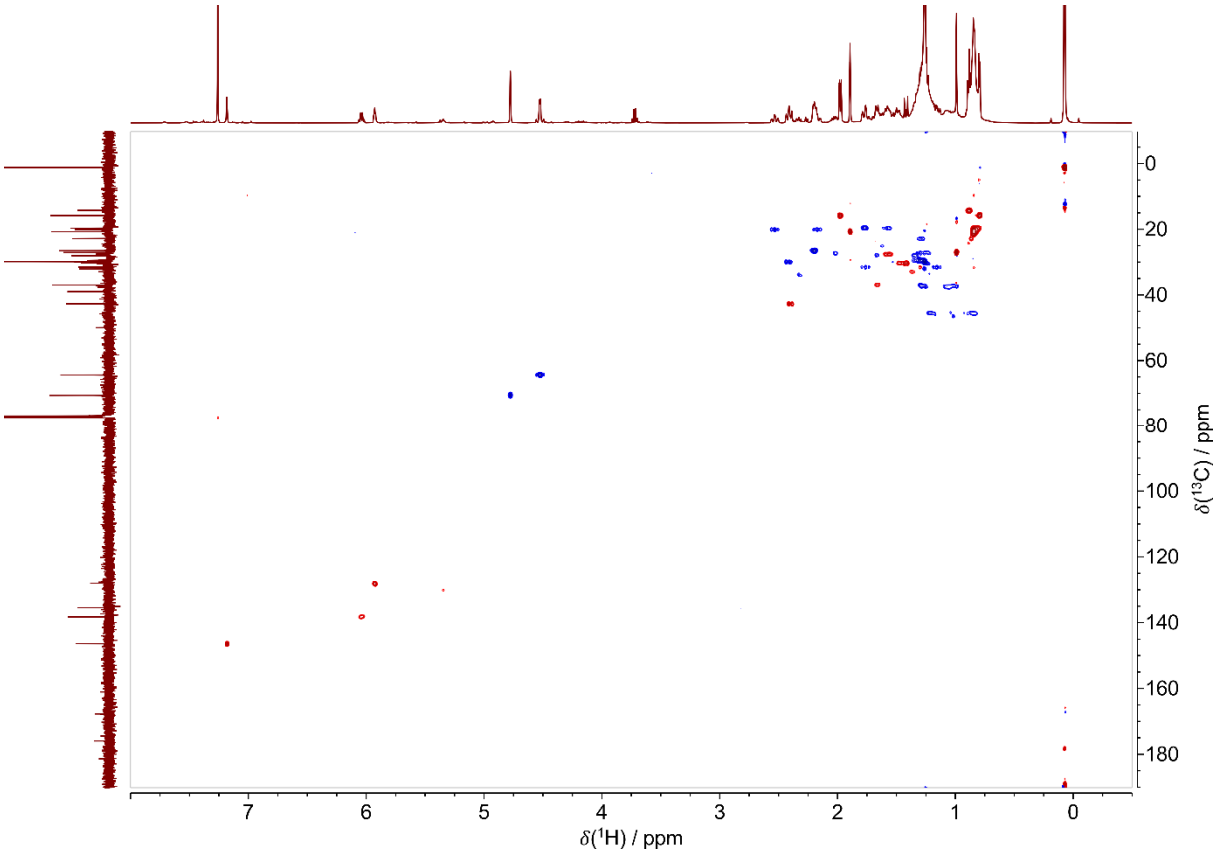


Figure S33. $^{1}H–^{13}C$ edHSQC NMR spectrum of solidagoic acid D (**3**) ($CDCl_3$, 500/126 MHz).

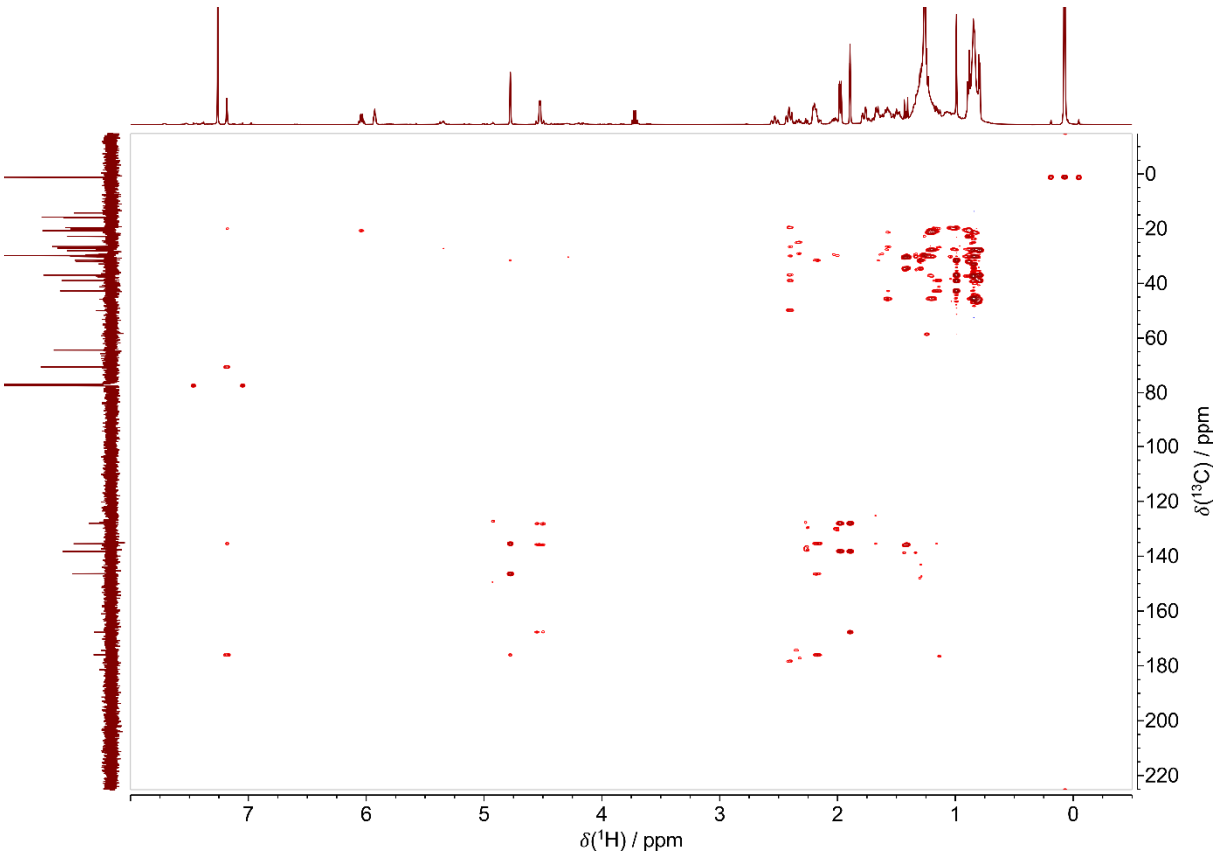


Figure S34. $^{1}H–^{13}C$ HMBC NMR spectrum of solidagoic acid D (**3**) ($CDCl_3$, 500/126 MHz).

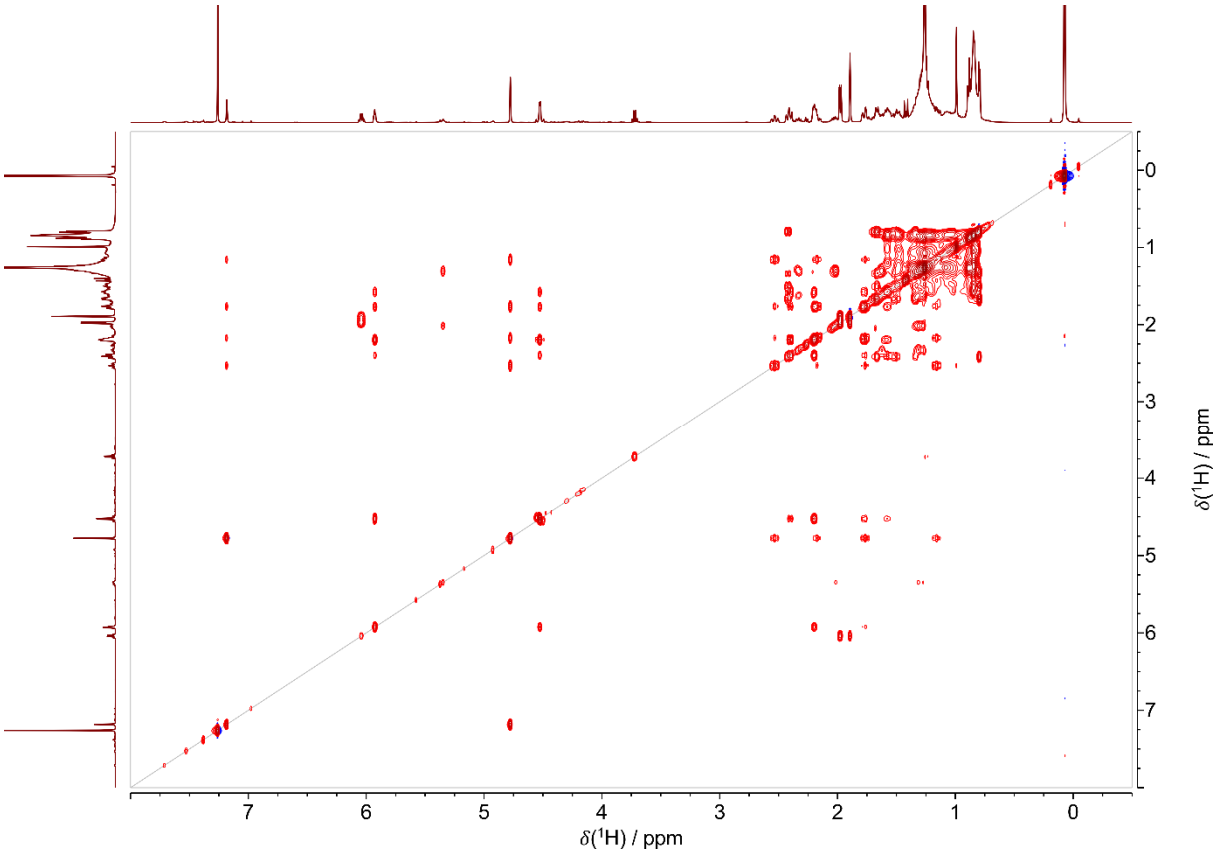


Figure S35. ^{1}H–^{1}H TOCSY NMR spectrum of solidagoic acid D (**3**) ($CDCl_3$, 500 MHz).

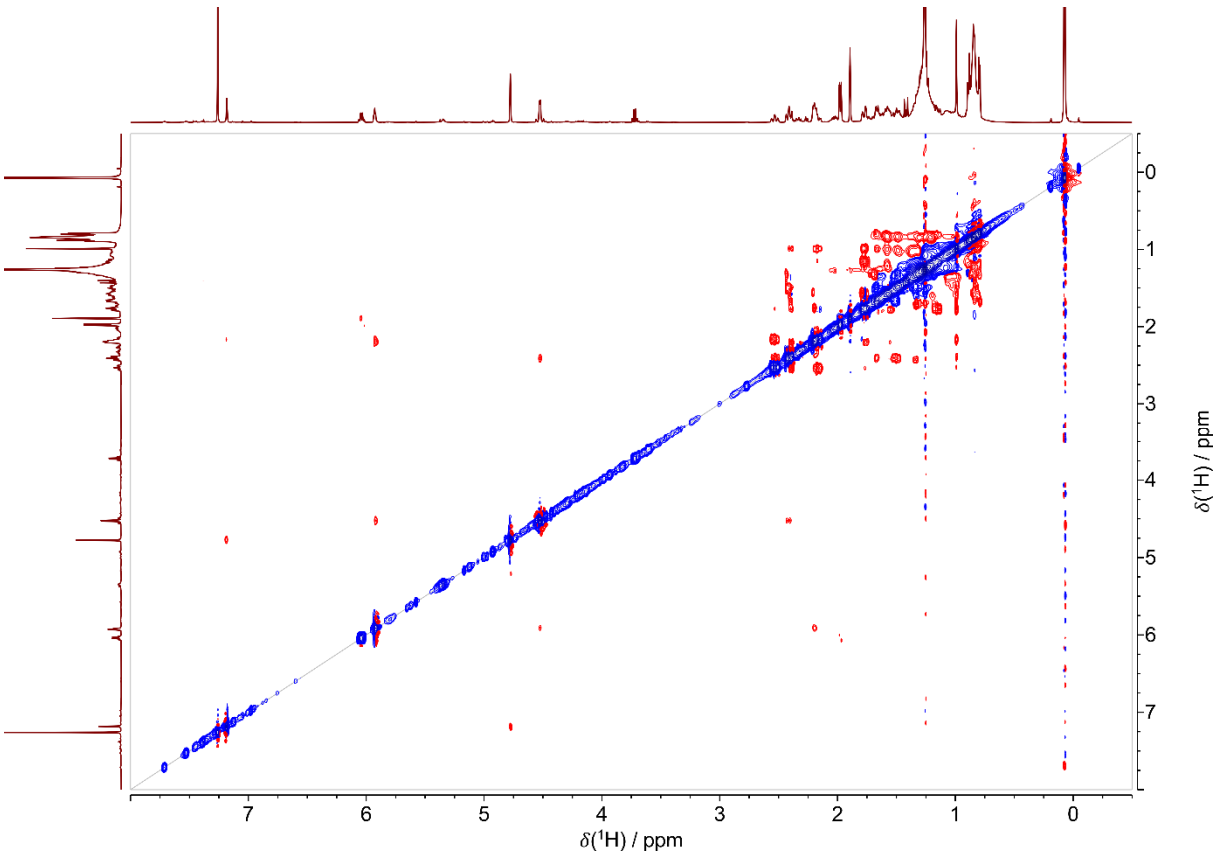


Figure S36. ^{1}H–^{1}H ROESY NMR spectrum of solidagoic acid D (**3**) ($CDCl_3$, 500 MHz).

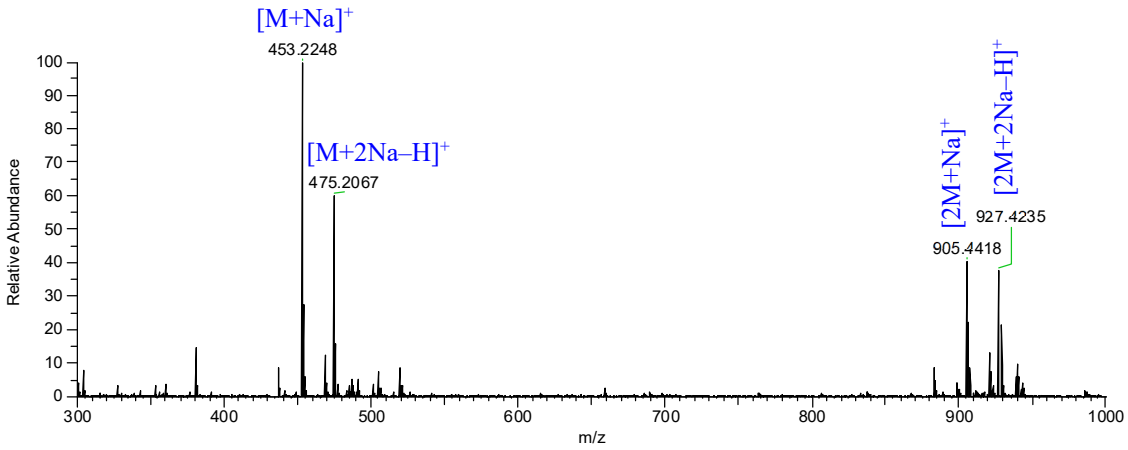


Figure S37. HR-ESI$^+$-MS spectrum of solidagoic acid D (**3**), *m/z* 453.2247 $[M+Na]^+$ (calculated for $C_{25}H_{34}O_6Na^+$, *m/z* 453.2248 $[M+Na]^+$, error: 0.1 ppm).

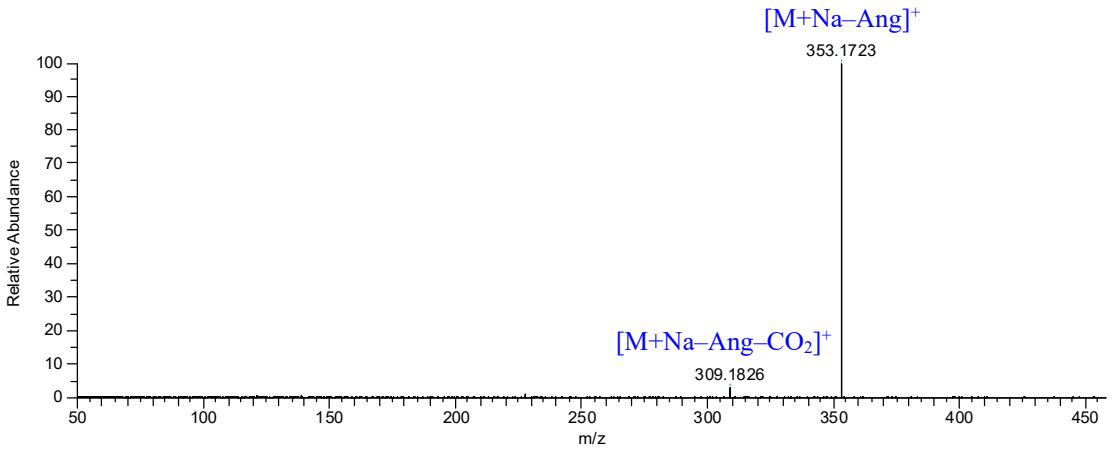


Figure S38. HR-ESI$^+$-MS/MS of solidagoic acid D (**3**) with a normalized HCD collision energy of 20%. Precursor ion: *m/z* 453.2248 $[M+Na]^+$, $C_{25}H_{34}O_6Na^+$. Ang denotes an angelate group ($C_5H_8O_2$).

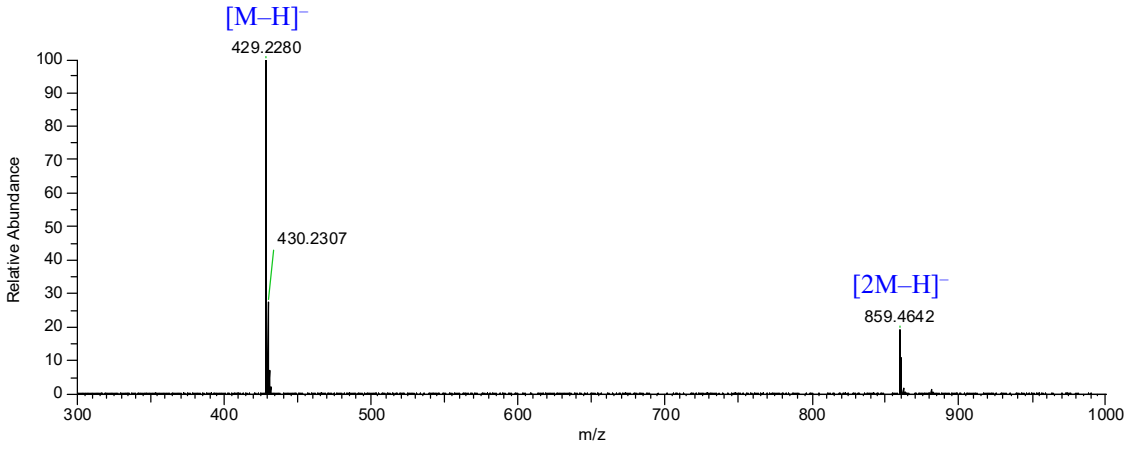


Figure S39. HR-ESI$^-$-MS spectrum of solidagoic acid D (**3**), *m/z* 429.2280 $[M–H]^-$ (calculated for $C_{25}H_{33}O_6^-$, *m/z* 429.2283 $[M–H]^-$, error: –0.5 ppm).

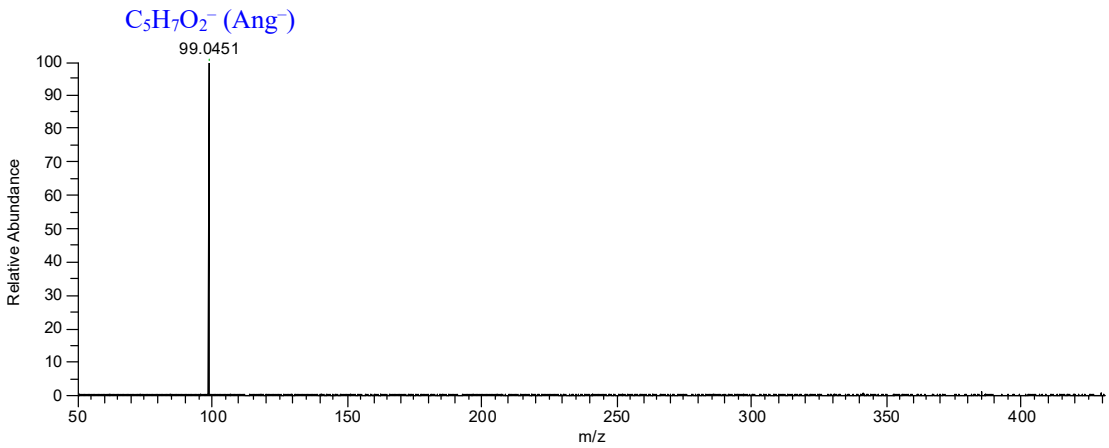


Figure S40. HR-ESI$^-$-MS/MS of solidagoic acid D (**3**) with a normalized HCD collision energy of 50%. Precursor ion: *m*/*z* 429.2283 $[M–H]^-$, $C_{20}H_{27}O_4^-$. Ang$^-$ denotes an angelate ion.

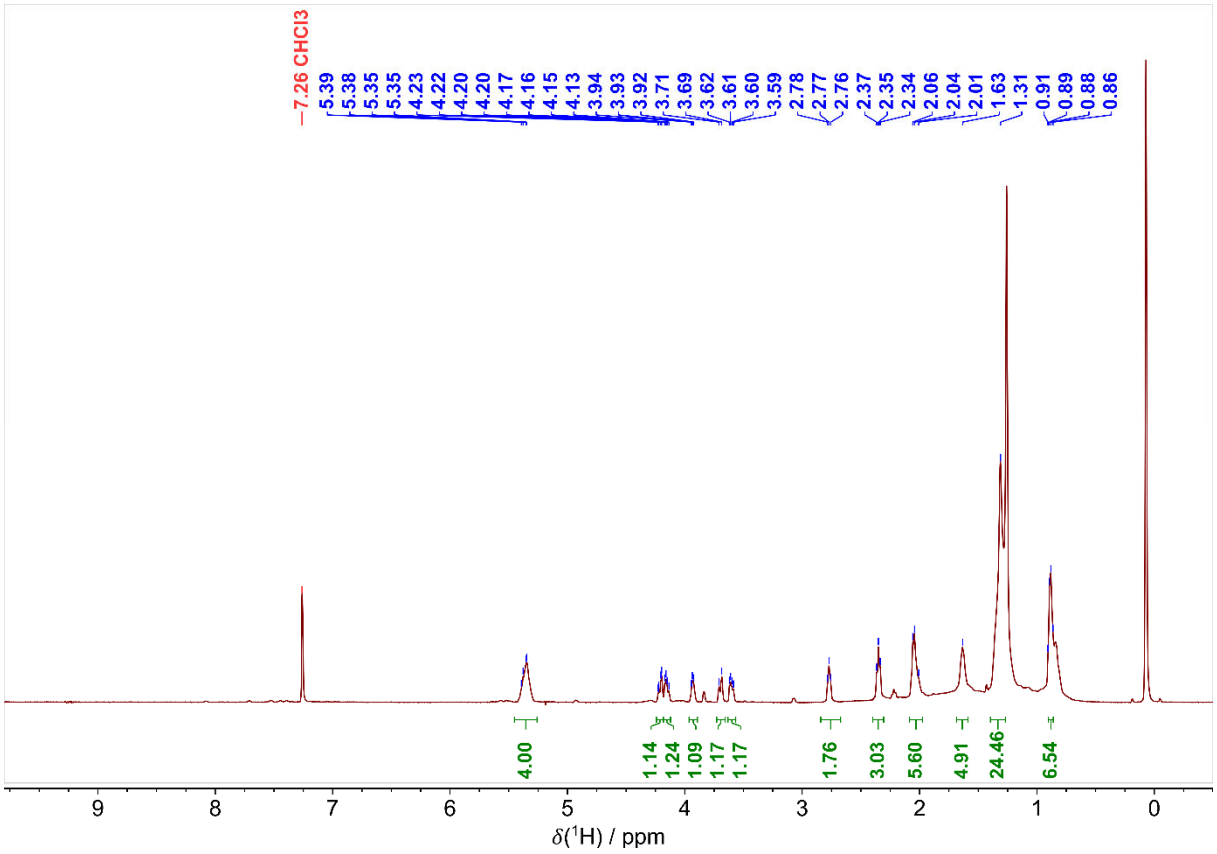


Figure S41. ^{1}H NMR spectrum of 1-linoleoyl glycerol (**4**) ($CDCl_3$, 500 MHz).

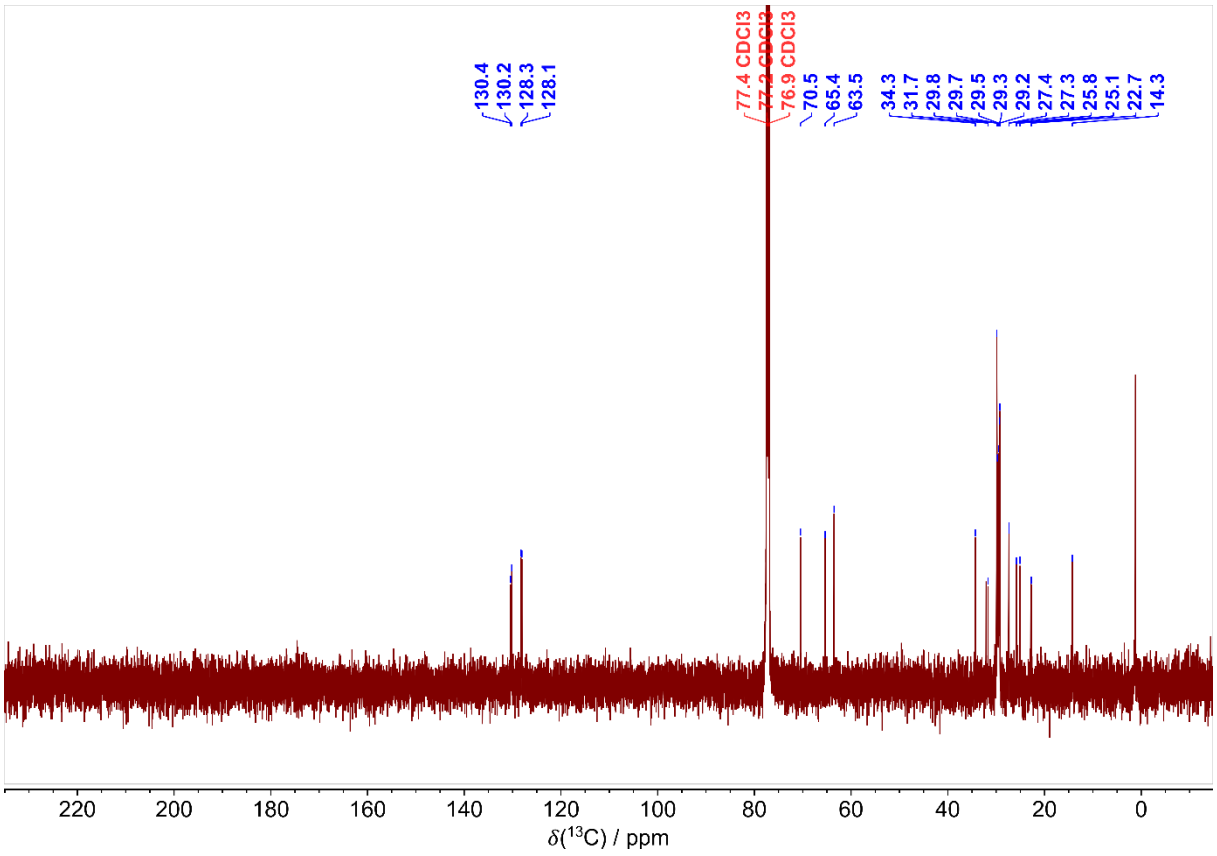


Figure S42. ^{13}C NMR spectrum of 1-linoleoyl glycerol (**4**) ($CDCl_3$, 126 MHz).

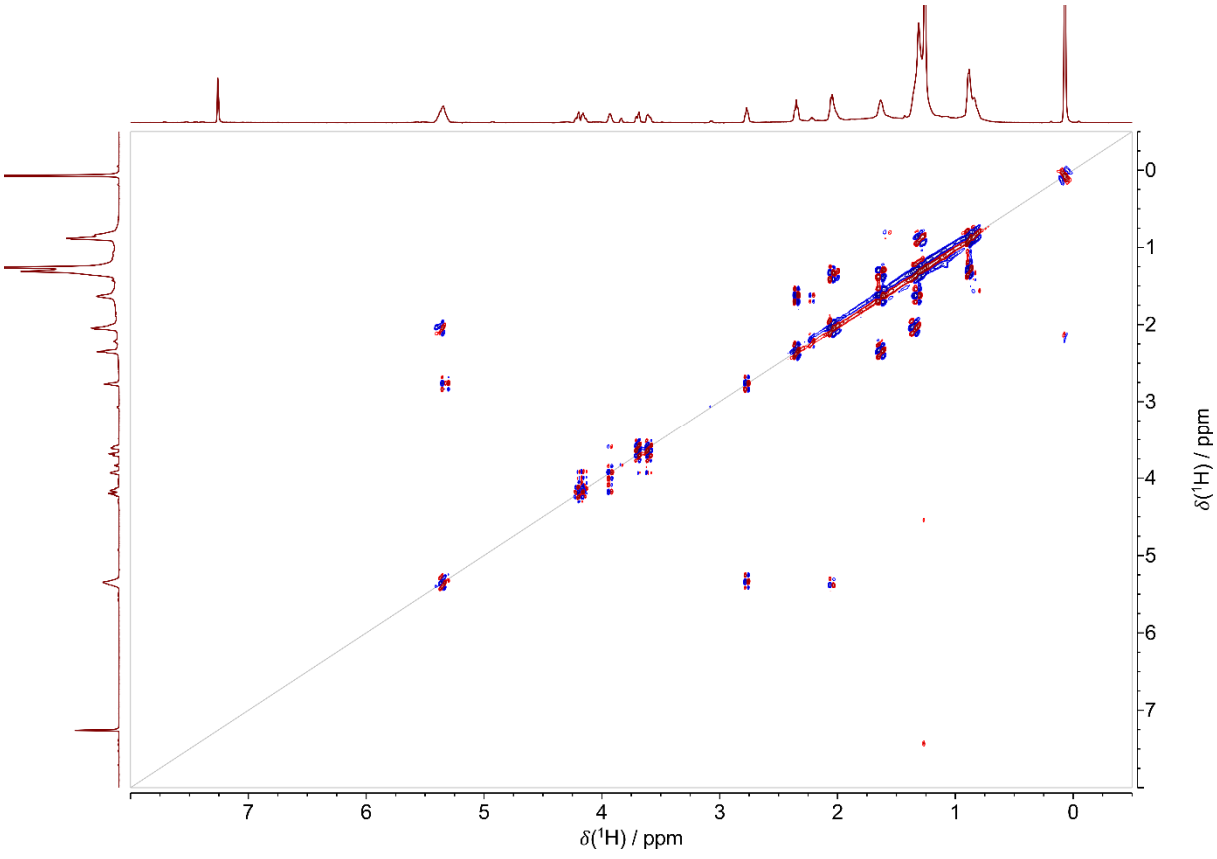


Figure S43. ^{1}H–^{1}H DQF-COSY NMR spectrum of 1-linoleoyl glycerol (**4**) ($CDCl_3$, 500 MHz).

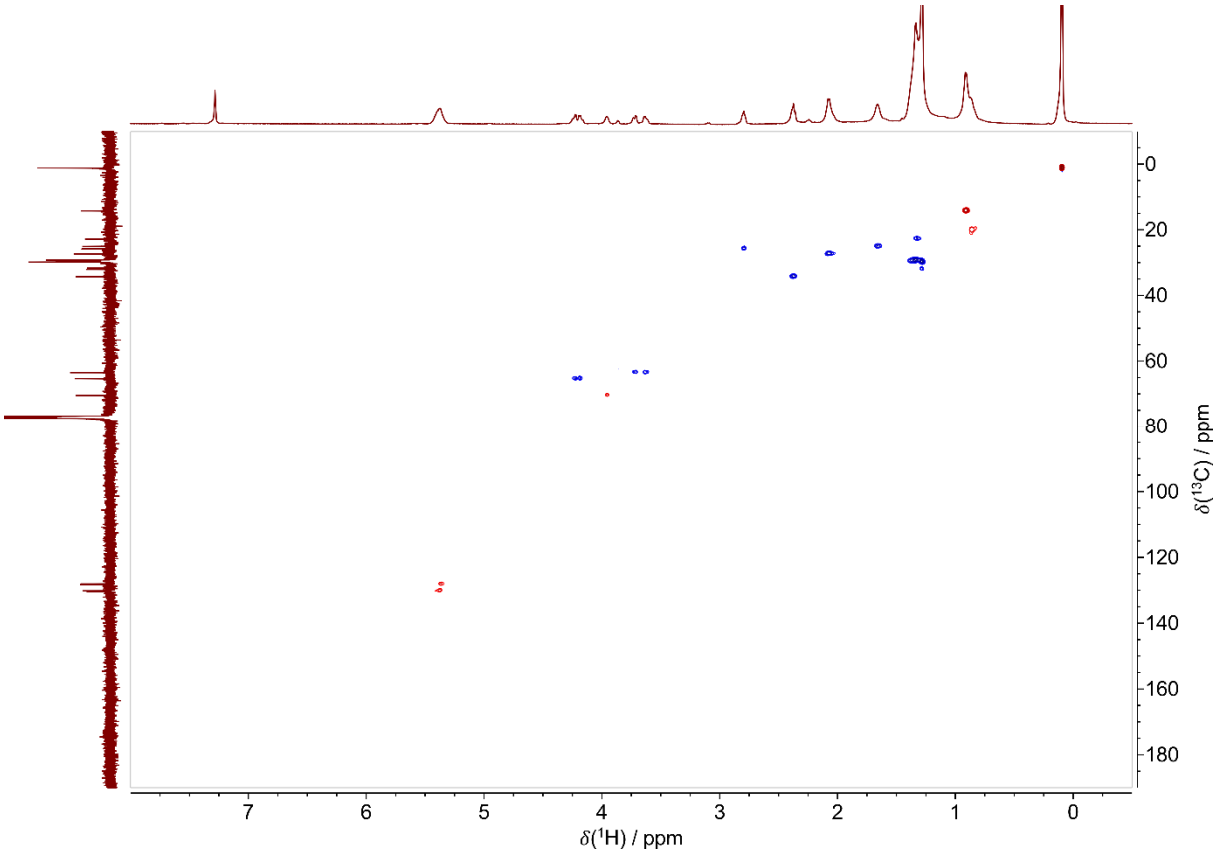


Figure S44. $^{1}H–^{13}C$ edHSQC NMR spectrum of 1-linoleoyl glycerol (**4**) ($CDCl_3$, 500/126 MHz).

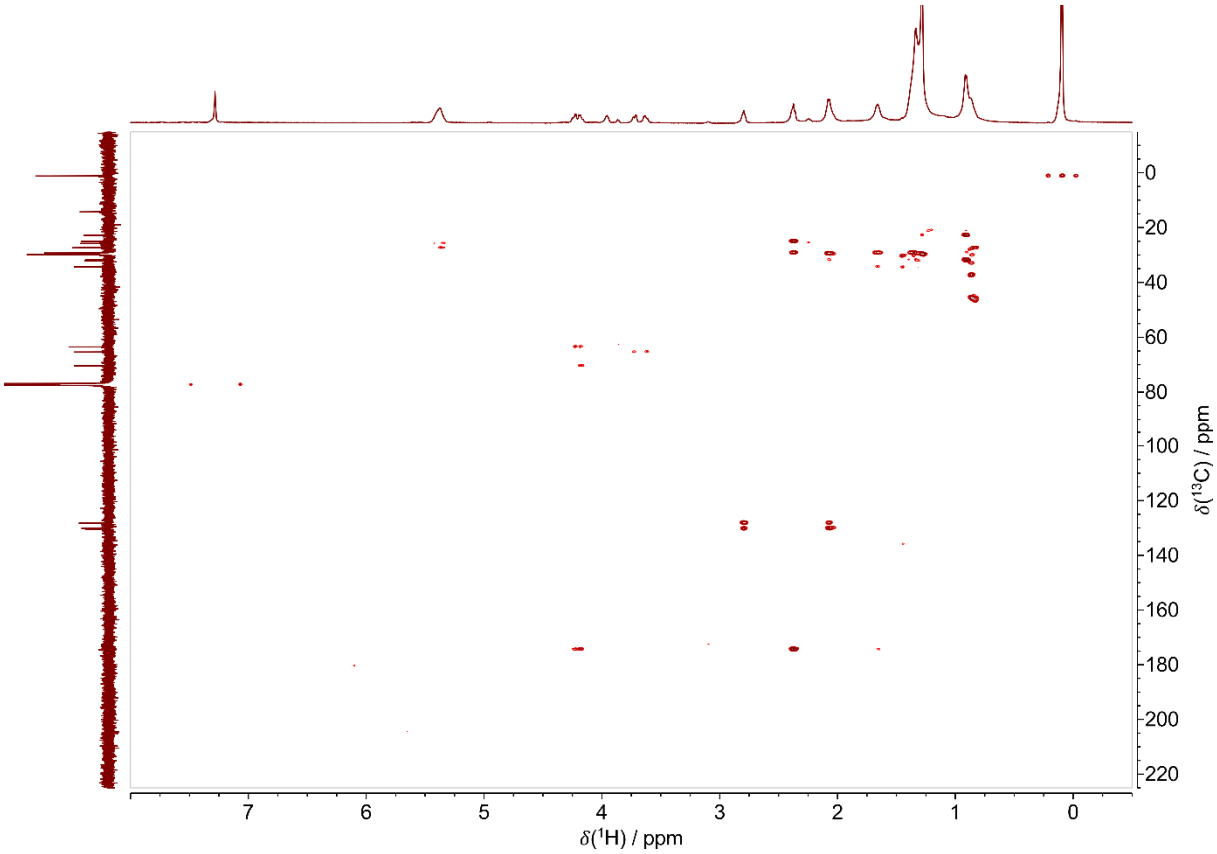


Figure S45. $^{1}H–^{13}C$ HMBC NMR spectrum of 1-linoleoyl glycerol (**4**) ($CDCl_3$, 500/126 MHz).

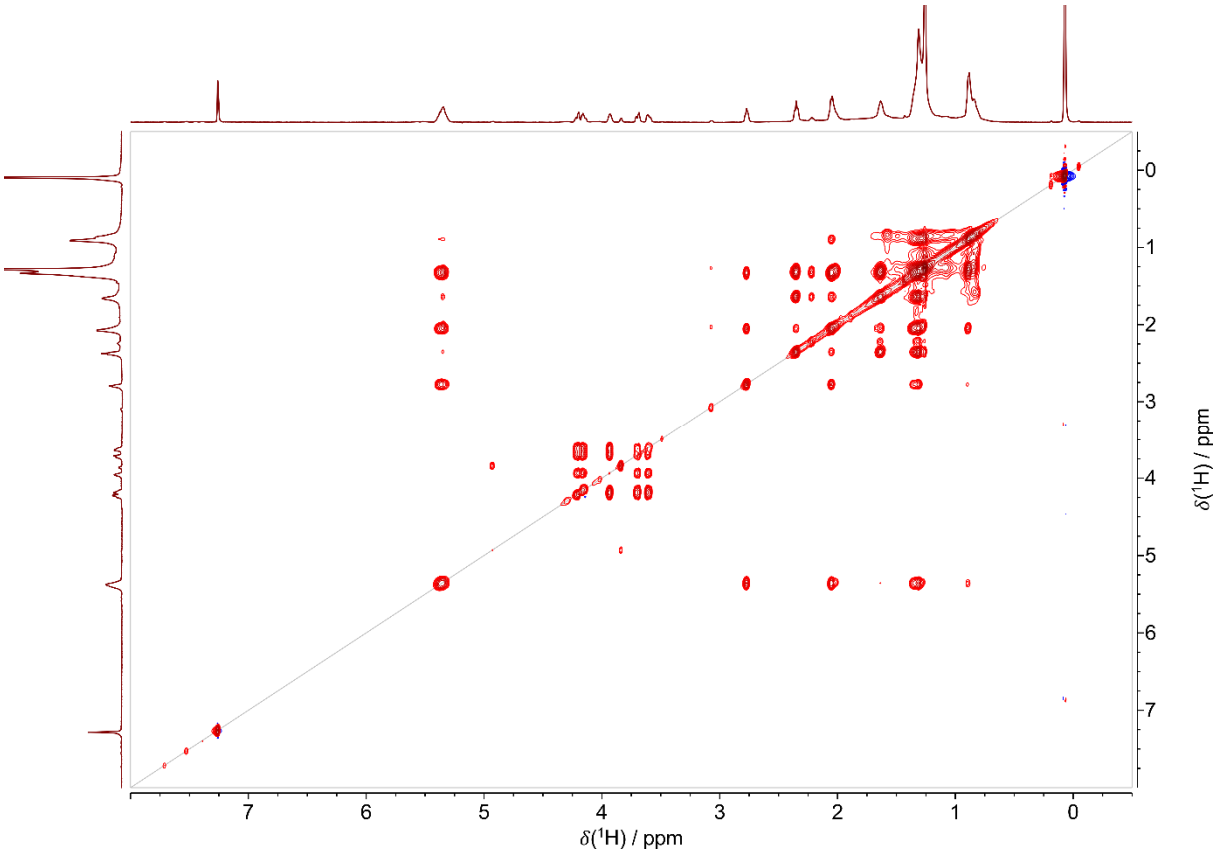


Figure S46. ^{1}H–^{1}H TOCSY NMR spectrum of 1-linoleoyl glycerol (**4**) ($CDCl_3$, 500 MHz).

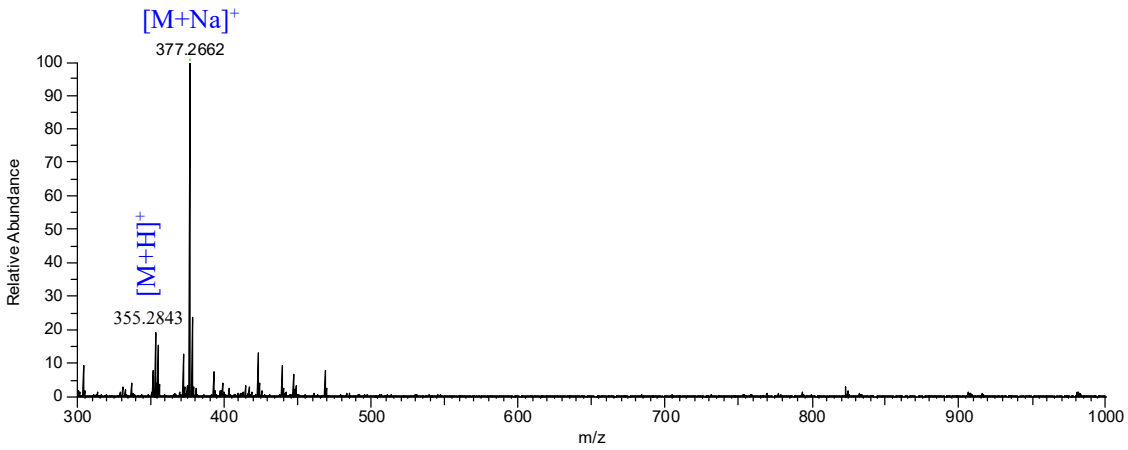


Figure S47. HR-ESI^{+}-MS spectrum of 1-linoleoyl glycerol (**4**), *m/z* 377.2662 $[M+Na]^{+}$ (calculated for $C_{21}H_{38}O_4Na^{+}$, *m/z* 377.2662 $[M+Na]^{+}$, error: 0.0 ppm); *m/z* 355.2843 $[M+H]^{+}$ (calculated for $C_{21}H_{39}O_4^{+}$, *m/z* 355.2843 $[M+H]^{+}$, error: 0.0 ppm).

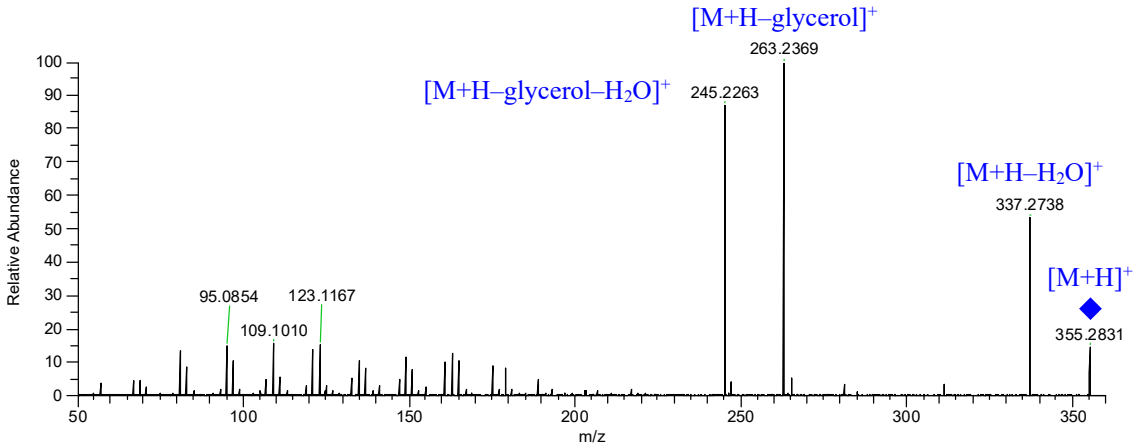


Figure S48. HR-ESI$^+$-MS/MS of 1-linoleoyl glycerol (**4**) with a normalized HCD collision energy of 50%. Precursor ion: *m/z* 355.2831 $[M+H]^+$, $C_{21}H_{39}O_4^+$.

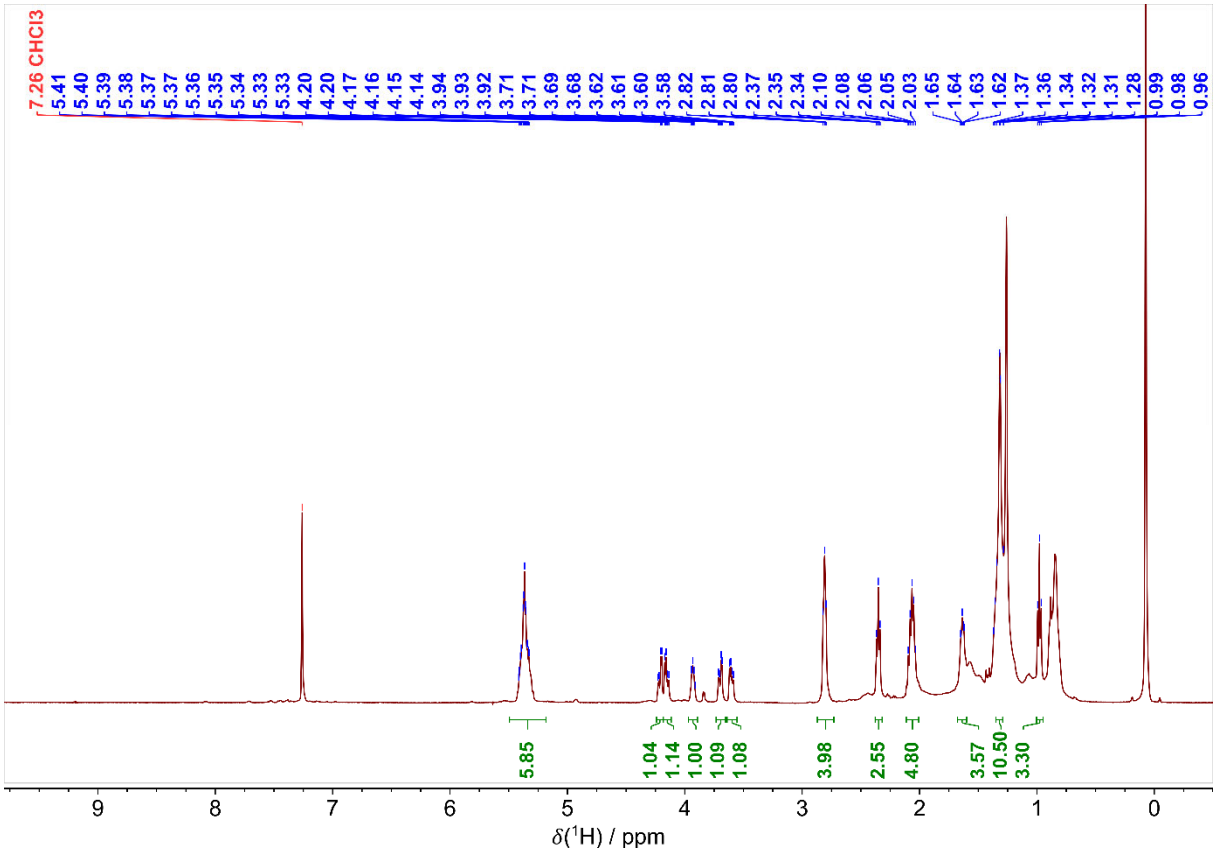


Figure S49. ^{1}H NMR spectrum of 1-α-linolenoyl glycerol (**5**) ($CDCl_3$, 500 MHz).

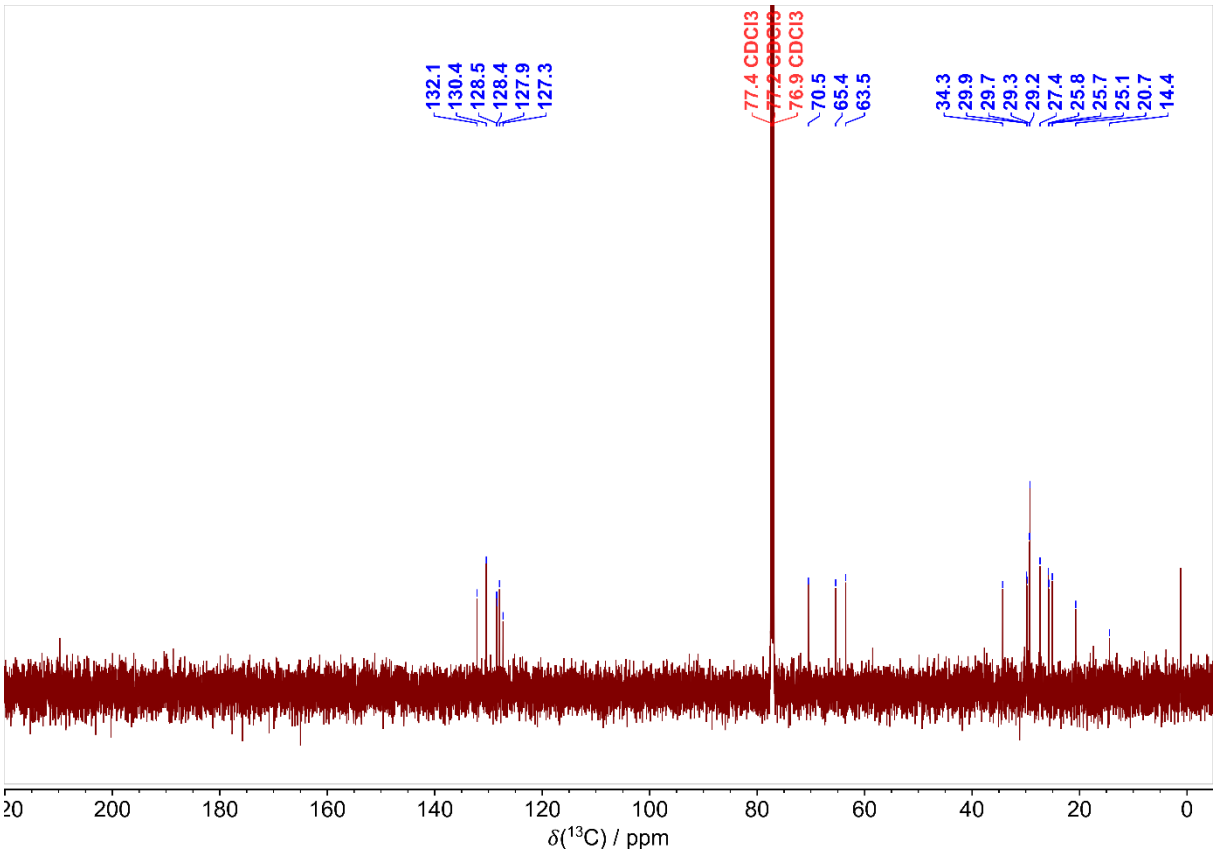


Figure S50. ^{13}C NMR spectrum of 1-α-linolenoyl glycerol (**5**) ($CDCl_3$, 126 MHz).

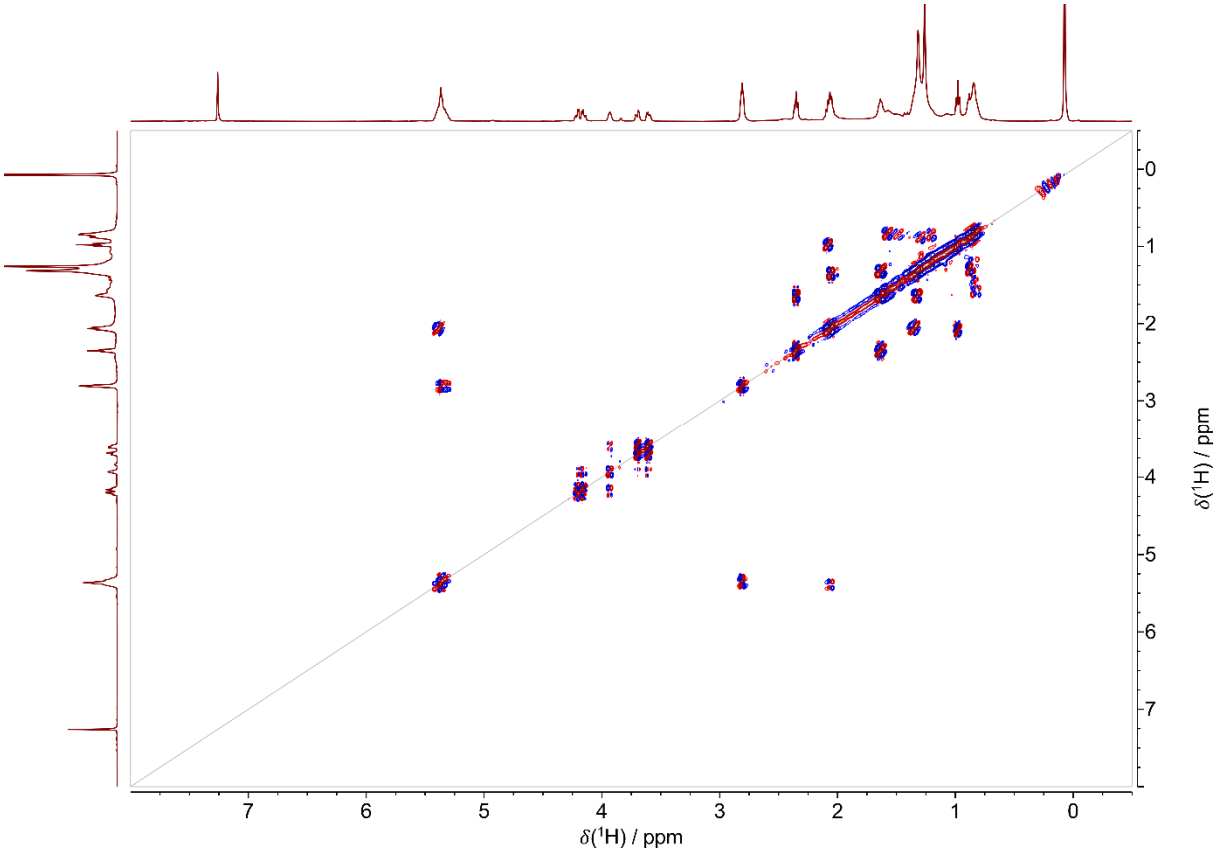


Figure S51. ^{1}H–^{1}H DQF-COSY NMR spectrum of 1-α-linolenoyl glycerol (**5**) ($CDCl_3$, 500 MHz).

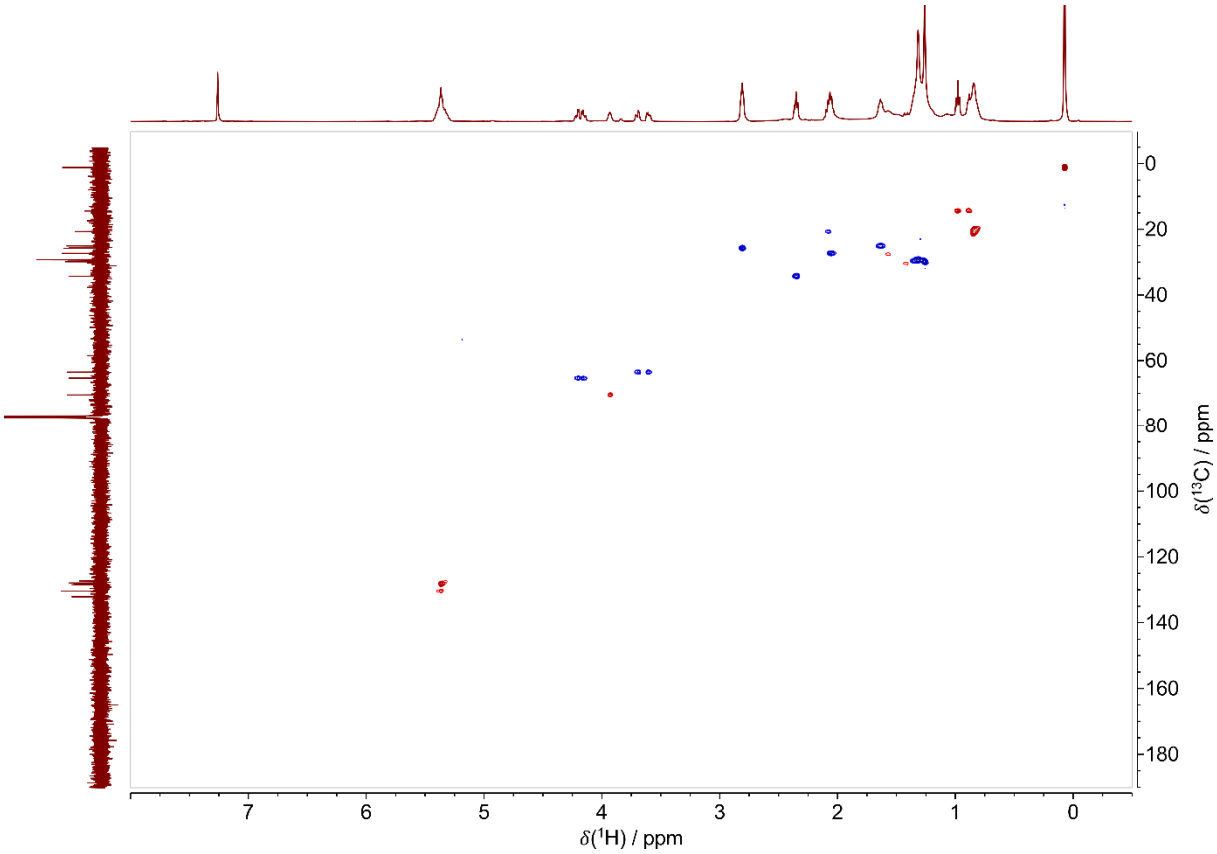


Figure S52. $^{1}H–^{13}C$ edHSQC NMR spectrum of 1-α-linolenoyl glycerol (**5**) ($CDCl_3$, 500/126 MHz).

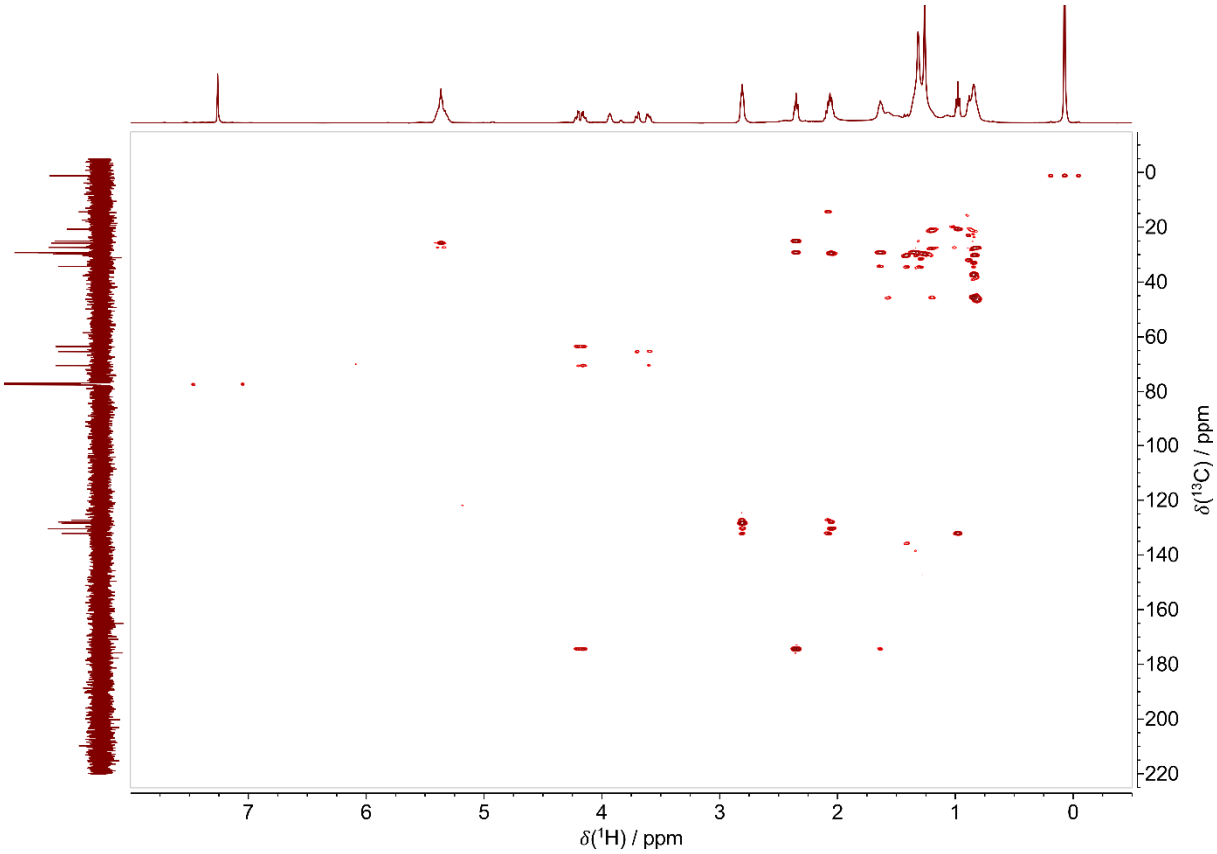


Figure S53. $^{1}H–^{13}C$ HMBC NMR spectrum of 1-α-linolenoyl glycerol (**5**) ($CDCl_3$, 500/126 MHz).

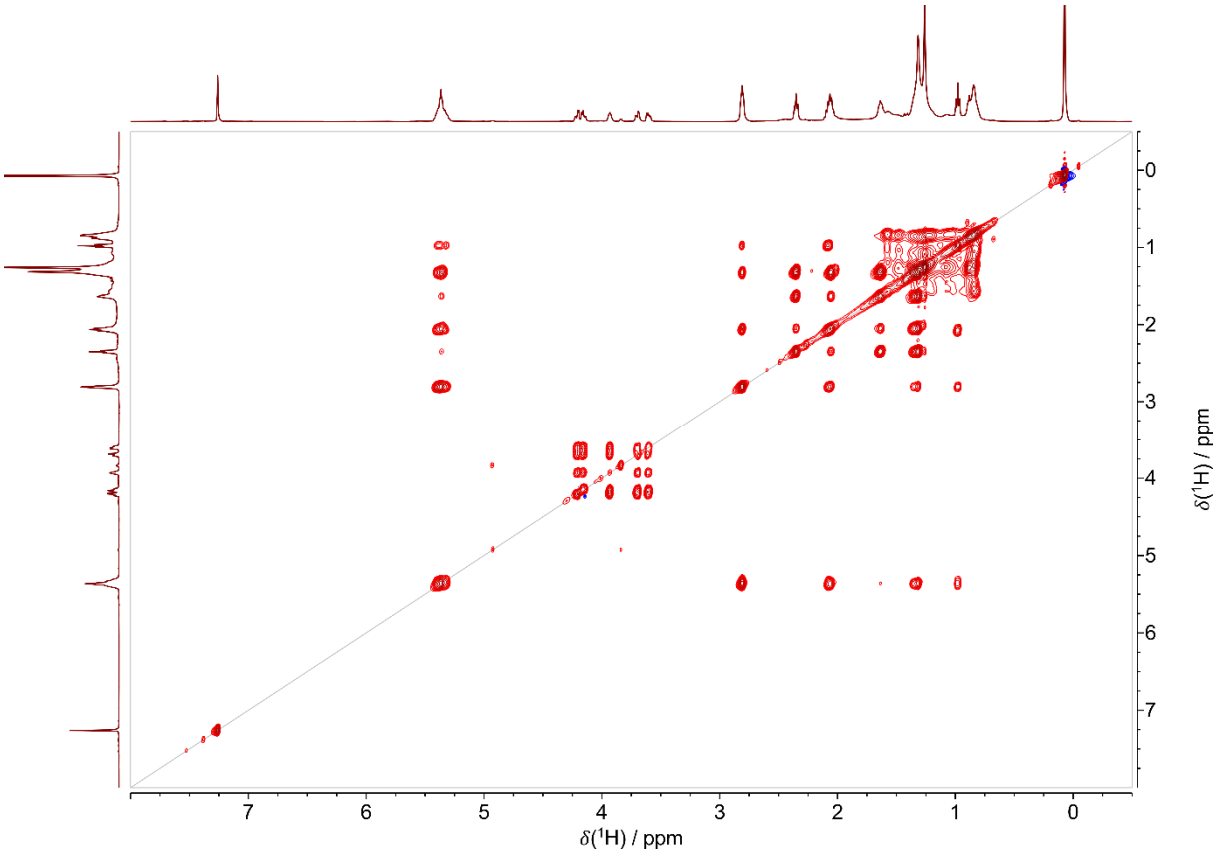


Figure S54. ^{1}H–^{1}H TOCSY NMR spectrum of 1-α-linolenoyl glycerol (**5**) ($CDCl_3$, 500 MHz).

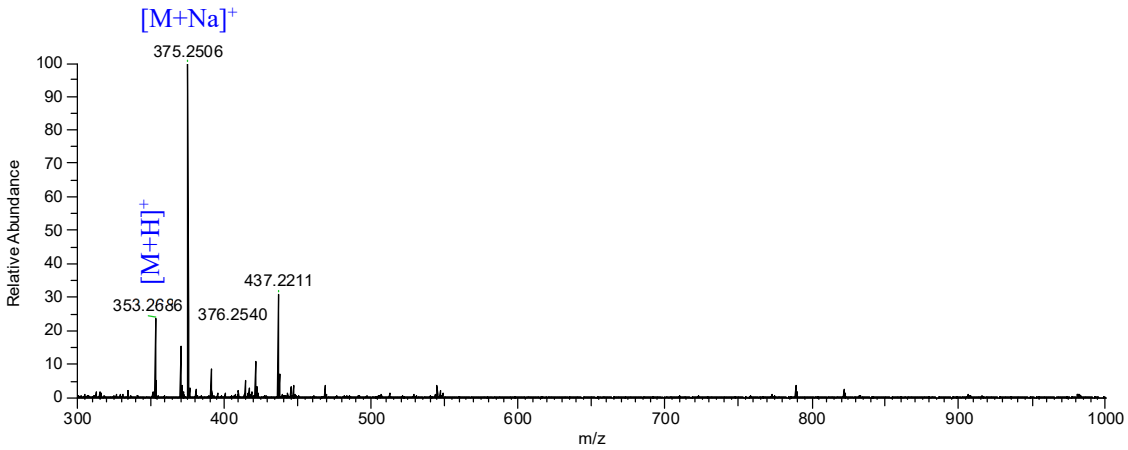


Figure S55. HR-ESI^{+}-MS spectrum of 1-α-linolenoyl glycerol (**5**), *m/z* 375.2506 $[M+Na]^{+}$ (calculated for $C_{21}H_{36}O_4Na^{+}$, *m/z* 375.2506 $[M+Na]^{+}$, error: 0.0 ppm); *m/z* 353.2686 $[M+H]^{+}$ (calculated for $C_{21}H_{37}O_4^{+}$, *m/z* 353.2686 $[M+H]^{+}$, error: 0.0 ppm).

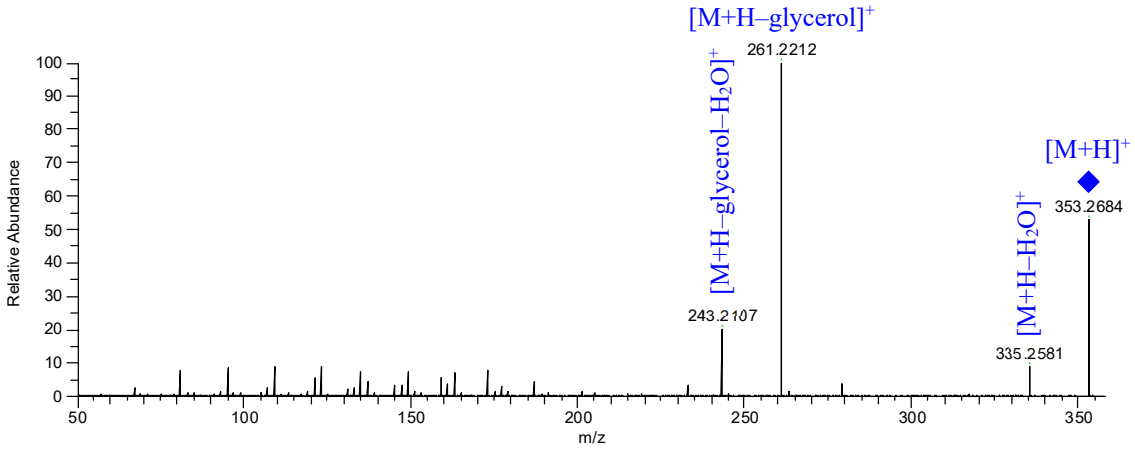


Figure S56. HR-ESI$^+$-MS/MS of 1-α-linolenoyl glycerol (**5**) with a normalized HCD collision energy of 50%. Precursor ion: *m/z* 353.2684 $[M+H]^+$, $C_{21}H_{37}O_4^+$.